

Original Article

Cite this article: Xiong C, Niu Y, Chen H, Chen A, Zhang C, Li F, Yang S, and Xu S (2019) Detrital zircon U–Pb geochronology and geochemistry of late Neoproterozoic – early Cambrian sedimentary rocks in the Cathaysia Block: constraint on its palaeo-position in Gondwana supercontinent. *Geological Magazine* **156**: 1587–1604. <https://doi.org/10.1017/S0016756819000013>


Received: 1 August 2018
Revised: 24 November 2018
Accepted: 4 January 2019
First published online: 6 March 2019

Keywords:

provenance; tectonic setting; detrital zircon; Cathaysia Block; Gondwana

Author for correspondence: Chen Xiong and Anqing Chen, Emails: xiongchen105@163.com and aqinchen@163.com

Detrital zircon U–Pb geochronology and geochemistry of late Neoproterozoic – early Cambrian sedimentary rocks in the Cathaysia Block: constraint on its palaeo-position in Gondwana supercontinent

Chen Xiong^{1,2,*} , Yaoling Niu^{2,3}, Hongde Chen^{1,4}, Anqing Chen^{1,4,*}, Chenggong Zhang¹, Feng Li^{1,5}, Shuai Yang¹ and Shenglin Xu¹

¹Institute of Sedimentary Geology, Chengdu University of Technology, Chengdu 610059, China; ²Department of Earth Sciences, Durham University, Durham DH1 3LE, United Kingdom; ³Institute of Oceanology, Chinese Academy of Sciences, Qingdao 266071, China; ⁴State Key Laboratory of Oil and Gas Reservoir Geology and Exploitation, Chengdu University of Technology, Chengdu 610059, China and ⁵The No. 3 Gas Production Plant, SINOPEC Southwest China Oil and Gas Company, Deyang, China

Abstract

We present updated U–Pb ages and Hf isotopic compositions of detrital zircons and whole-rock geochemical data to investigate the provenance and tectonic setting of late Neoproterozoic and early Cambrian sandstones from the Cathaysia Block, in order to offer new constraints on its tectonic evolution and its palaeo-position within the supercontinent. The source rocks for the studied sandstones were dominated by felsic–intermediate materials with moderate weathering history. U–Pb dating results show major populations at c. 2500 Ma, 1000–900 Ma and 870–716 Ma with subordinate peaks at 655–532 Ma, consistent with the global Neoproterozoic continental crust growth, assembly and break-up of Rodinia, and Pan-African Event associated with the formation of Gondwana. Zircon U–Pb ages and Hf isotopic data suggest that most derived from exotic terranes once connected to the Cathaysia Block. Using whole-rock geochemical analysis, it was determined that the studied sedimentary rocks were deposited in a passive continental margin and the Cathaysia and Yangtze blocks were part of the same continent; no Cambrian ocean existed between them. Compiling a detrital zircon dataset from Qiangtang, northern India, the Lhasa Terrane and Western Australia, the Cathaysia Block seems to be more similar to the Qiangtang and western part of the northern India margin, instead of having a direct connection with the Lhasa Terrane and Western Australia in the Gondwana reconstruction during the late Neoproterozoic and Cambrian eons.

1. Introduction

The break-up of the Rodinia supercontinent is known to have led to some fragments accreting to form Gondwana during late Precambrian and early Palaeozoic time. However, the palaeo-position of the Cathaysia Block within the Gondwana supercontinent, or whether it even belonged to Gondwana, remains a matter of debate (Cawood *et al.* 2007, 2013; Li *et al.* 2010, 2014; Duan *et al.* 2011; Yao *et al.* 2011, 2014; Wang *et al.* 2013; Xu *et al.* 2013, 2016). Diverse configuration relationships over the past decades have been proposed for the location of the Cathaysia Block during the assembly of Gondwana (Yu *et al.* 2008, 2012; Wang *et al.* 2010; Duan *et al.* 2011; Yao *et al.* 2011, 2014; Cawood *et al.* 2013; Li *et al.* 2014; Xu *et al.* 2014a). Palaeomagnetic records show that the South China Block (SCB) should have been near western/northwestern Australia and the India–Himalaya region of the Gondwana margin (Metcalf, 1996; Yang *et al.* 2004; Zhang *et al.* 2015). Stratigraphic correlations indicate that the SCB was most likely linked to northwestern India during the late Neoproterozoic Era, and then separated from India and moved to northwestern Australia during the early Cambrian Period (Yu *et al.* 2012; Jiang *et al.* 2013). By comparing the polar position derived from the early Palaeozoic sedimentary rocks to previously documented poles of the Yangtze Block (Huang *et al.* 2000), Yang *et al.* (2004) proposed that the SCB should have been near Western Australia. However, Li *et al.* (2004) argued that the SCB was a discrete continental block in the palaeo-Pacific and separated from Laurentia during early Cambrian time, suggesting the SCB was not part of early Palaeozoic Gondwana. At present, most researchers are focusing their studies on the igneous rocks and magmatic events of the SCB, whereas studies of the late Neoproterozoic – Palaeozoic sedimentary rocks are comparatively less common because of extensive Phanerozoic reworking. The composition of the sedimentary rocks records

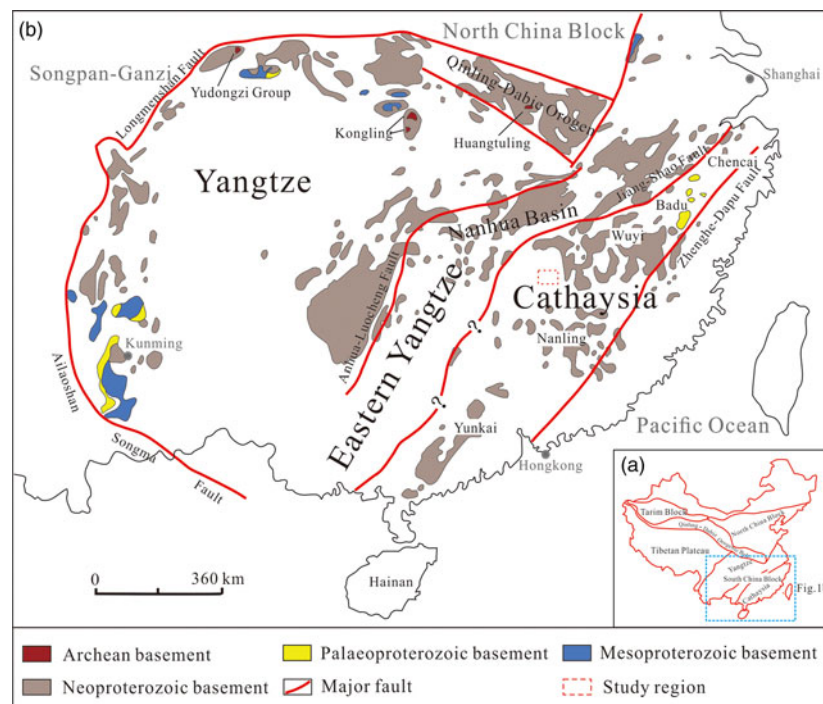


Fig. 1. (Colour online) (a) Tectonic outline of China and (b) geological map of South China Block showing the distribution of Precambrian rocks in the Yangtze and Cathaysia blocks and the study region (modified after Zhao & Cawood, 2012).

important information to determine their source regions, tectonic settings and affinity with other blocks, providing additional information to understand the tectonic evolution of the Cathaysia Block and its palaeo-position within the supercontinents.

Zircon is the most effective accessory mineral for geochronology because it is common in rocks and is resistant to physical and chemical alteration (Fedo *et al.* 2003). The geochemical composition of sedimentary rocks can be a suitable indicator of the characteristics of the source rocks and tectonic settings (e.g. Nesbitt & Young, 1982; Bhatia, 1983; Bhatia & Crook, 1986; Fedo *et al.* 1995). Systematic dating of detrital zircons and geochemical analysis can therefore show the tectonic histories of the Cathaysia Block and its palaeo-position within the supercontinents (Shu *et al.* 2011, 2014; Yu *et al.* 2012; Cawood *et al.* 2013; Xu *et al.* 2014a). Together with the abundant updated detrital zircon datasets that have been reported in relevant blocks, we present new U–Pb–Hf isotopes of detrital zircons and whole-rock geochemical data from late Neoproterozoic – early Cambrian sedimentary rocks in the western Cathaysia Block. We compare these data with those of age-equivalent sedimentary rocks in relevant regions including Qiangtang, northern India, Lhasa Terrane and Western Australia to evaluate the source-area characteristics and to determine the provenance and tectonic settings of the sedimentary rocks; based on these data, we offer new constraints on the palaeo-position of the Cathaysia Block within the Gondwana supercontinent.

2. Geological setting

The North and South China blocks are the two largest Precambrian domains in eastern continental China. The SCB consists of the Cathaysia Block to the SE and the Yangtze Block to the NW (Fig. 1a) separated by the Jiang–Shao Fault (JSF) in the east; its western extension is however unclear because of younger tectonic modifications

(Fig. 1b; Guo *et al.* 1985; Zhao & Cawood, 2012). The two blocks have different Precambrian crustal evolution histories with contrasting crystalline basement rocks. The Yangtze Block is mainly composed of a small amount of Archean–Palaeoproterozoic crystalline basement, surrounded by Neoproterozoic orogens. Archean basement rocks have only been reported in the northern part of the Yangtze Block, represented by the Yudongzi Group, Kongling Complex and Huangtuling granulites, while Palaeoproterozoic basement rocks are sparsely exposed along its western margin (Fig. 1b; Zhou *et al.* 2002; Zhao & Cawood, 2012; Xia *et al.* 2015). The Kongling Complex is the oldest basement of the SCB, predominantly consisting of Archean tonalite–trondhjemite–granodiorite (TTG) gneisses with varying ages of 2.7–3.3 Ga (Gao *et al.* 2011). The Precambrian basement rocks in the Cathaysia Block are only reported from Chencai, Badu, Wuyishan, Nanling and Yunkai along a NE–SW belt bounded by the JSF to the NW and the Zhenghe–Dapu Fault to the SE (Fig. 1b; Zhao & Cawood, 2012). The oldest known crystalline rocks in it are 1.77–1.89 Ga granites and amphibolites from NE Cathaysia (Yu *et al.* 2009; Xia *et al.* 2012).

The SCB initially formed via the collision between the Cathaysia and Yangtze blocks during Neoproterozoic time, resulting in the Jiangnan Orogen (also termed the ‘Sibao’ Orogen) along the southeastern margin of the Yangtze Block (Guo *et al.* 1985). However, the timing of this collision remains under debate, varying over the late Mesoproterozoic – Neoproterozoic eras (Cawood *et al.* 2013; Wang *et al.* 2013; Xia *et al.* 2018). Following the amalgamation of the Cathaysia and Yangtze blocks to form a coherent cratonic block, the SCB underwent initial fragmentation during 830–720 Ma and then widespread rifting (Wang *et al.* 2012). The rift system mainly occurred within the central and western part of the craton, generating widespread bimodal igneous rocks and associated sedimentary successions (Yu *et al.* 2010; Xia *et al.* 2018). The Nanhua Rifting, the major Neoproterozoic rift system

in the SCB (Fig. 1b), ended during late Neoproterozoic time, with failed rift basins continuing to receive uppermost Neoproterozoic – lower Palaeozoic sediments (Yu *et al.* 2009).

The sedimentary patterns between the Cathaysia and Yangtze blocks are quite different during late Neoproterozoic and early Palaeozoic time. The central Yangtze Block is dominated by clastic rocks intercalated with carbonate (limestone and dolomite), siliciclastic and bimodal volcanic rocks and tillites in the Neoproterozoic units, and shale-silicite and carbonate rocks in the Cambrian strata. In contrast, the Cathaysia Block received massive siliciclastic sedimentation. The Neoproterozoic units are dominated by an association of mudstone, siltstone and (meta)sandstone intercalated with lenticular limestone, and the Cambrian units are dominated by mudstone and feldspathic sandstone intercalated with bioclastic limestone (BGMJRX, 1984; BGMRGX, 1985; BGMRHN, 1988; BGMRGZ, 1988; Liu & Xu, 1994; Chen *et al.* 2006; Wang *et al.* 2010). There is therefore a transition from a siliciclastic succession in the Cathaysia Block to a mixed siliciclastic and carbonate succession in the SE Yangtze Block across the SCB (Wang *et al.* 2010; Yao *et al.* 2014, 2015). During middle Palaeozoic time, a tectono-thermal event termed the Kwangian Orogeny occurred in the Cathaysia Block, resulting in high-temperature metamorphism, strong deformation (440–400 Ma) with widespread granitic intrusions, and a regional-scale unconformity between the pre-Devonian and Devonian strata (Shu *et al.* 2008; Wang *et al.* 2011; Xu *et al.* 2014a).

3. Sampling and methodology

A total of 13 sandstones including 10 from the early Cambrian strata and three from the late Neoproterozoic strata in the Jingganshan area underwent whole-rock geochemical analysis (Fig. 2; online Supplementary Table S1, available at <http://journals.cambridge.org/geo>). Of these, two samples were chosen for U–Pb geochronological and Hf isotopic analysis. Sample P40-01 is a grey fine-grained early Cambrian sandstone (Fig. 3a). Sample P43-01 is a greyish-brown, fine-grained late Neoproterozoic sandstone (Fig. 3c). Eleven thin-sections show that the clasts are angular to subangular, moderately to poorly sorted, and are immature in both composition and texture. The clastic mineralogy for sample P40-01 is dominated by quartz (89%) with minor feldspar (2%), lithic fragments (2%), mica (1%) and matrix (3%). The cements (3%), primarily silicate materials and calcite, are evenly distributed at grain contacts and between grain interstices (Fig. 3b). Sample P43-01 is composed of quartz (92%), feldspar (3%), lithic fragments (2%), matrix (3%) and silicate cements (2%) (Fig. 3d).

All the veins and weathering products were removed from the selected samples before cleaning and crushing into 200 mesh for geochemical analysis. Major and trace elements were respectively measured using X-ray fluorescence (XRF) and inductively coupled plasma – mass spectrometer (ICP-MS) at the Key Laboratory of Nuclear Techniques in Geosciences of Sichuan Province, Chengdu. The analytical precision was better than 5% for the major elements and 10% for all the trace elements, based on analysis of United States Geological Survey rock standards BIR-1, BCR-2 and BHVO-2.

Approximately 5 kg of representative material from each of the two samples were selected for zircon separation. Zircons were extracted using standard density and magnetic methods, and then handpicked under a binocular microscope. Representative zircons were mounted in epoxy resin and then polished and coated with gold. Transmitted, reflected and cathodoluminescence (CL)

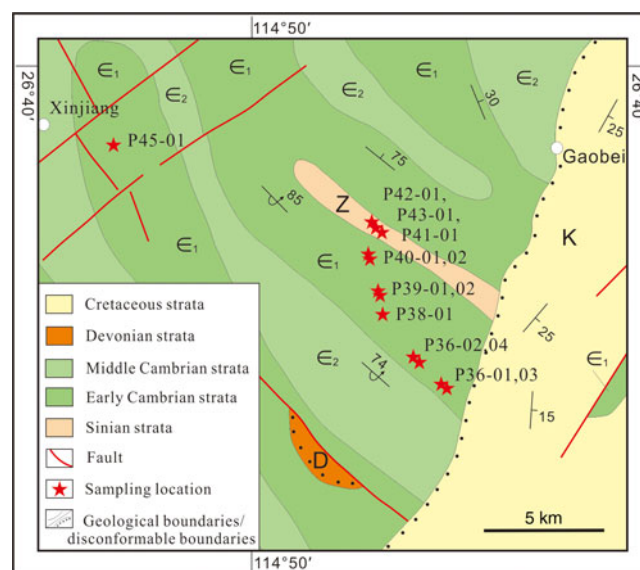


Fig. 2. (Colour online) Regional geological map and sampling localities in the Jingganshan area of the Cathaysia Block (modified after BGMJRX, 1984)

imaging was undertaken using an analytical scanning electron microscope (JSM IT100) connected to a Gatan MiniCL system. Zircon U–Pb isotopes were determined via laser ablation (LA-) ICP-MS at the Wuhan SampleSolution Analytical Technology Co. Ltd using an Agilent 7700e ICP-MS instrument equipped with a 193 nm COMPexPro 102 ArF excimer laser and a MicroLas optical system. The spot size and laser repetition rate were set to 32 μm and 5 Hz, respectively. Detailed instrumental conditions and analytical procedures are described in Zong *et al.* (2017) and Xiong *et al.* (2018). ICP-MS-DataCal (Liu *et al.* 2008) with zircon 91500 (recommended $^{206}\text{Pb}/^{238}\text{U}$ age of 1062.4 ± 0.8 Ma; Wiedenbeck *et al.* 1995) was used as an external standard for off-line data reduction. The analytical results of standard zircons 91500 are presented in online Supplementary Table S2 (available at <http://journals.cambridge.org/geo>), yielding weighted mean $^{206}\text{Pb}/^{238}\text{U}$ ages of 1062.4 ± 2.8 Ma (1σ , mean square weighted deviation or MSWD = 0.016, $n = 70$). Concordia diagrams and U–Pb ages were obtained using the Isoplot/Ex_ver3 (Ludwig, 2003) with 1σ errors. Zircon ages of more than 10% discordance were not included in the probability density distribution curves and the final interpretation. The data for concordant zircons including the U–Pb ages, Th/U ratios and trace-element compositions are listed in online Supplementary Tables S3 and S4. The $^{206}\text{Pb}/^{238}\text{U}$ ages were used for zircons younger than 1000 Ma, and the $^{207}\text{Pb}/^{206}\text{Pb}$ ages were used for zircons older than 1000 Ma (Griffin *et al.* 2004).

Hf isotopic analysis of the dated zircon grains was conducted using a Neptune Plus multi-collector (MC-) ICP-MS, in combination with a GeoLas 2005 excimer ArF laser ablation system, at the Wuhan SampleSolution Analytical Technology Co. Ltd. The instrumental conditions and detailed analytical procedure followed Hu *et al.* (2012). Standard zircon 91500 was used as an external standard to control the analytical accuracy. In this analysis, zircon standard 91500 yielded a weighted average $^{176}\text{Hf}/^{177}\text{Hf}$ ratio of 0.282308 ± 0.0000037 (2σ , MSWD = 0.13, $n = 26$; online Supplementary Table S5), consistent with the recommended $^{176}\text{Hf}/^{177}\text{Hf}$ ratios of 0.282308 ± 0.000006 (Blichert-Toft, 2008). The initial $^{176}\text{Hf}/^{177}\text{Hf}$ ratio values were calculated based on the decay constant of ^{176}Lu of $1.867 \times 10^{-11} \text{ year}^{-1}$ (Söderlund *et al.*

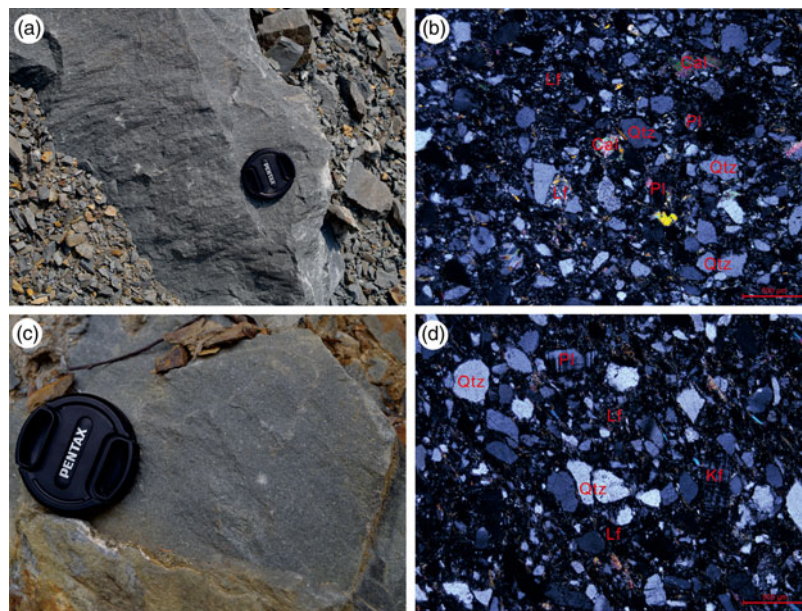


Fig. 3. (Colour online) Representative field photographs and photomicrographs: (a, b) early Cambrian fine-grained sandstone (sample P40-01); (c, d) late Neoproterozoic fine-grained sandstone (sample P43-01). Cal – calcite; Lt – lithic fragment; Kf – K-feldspar; Pl – plagioclase; Qtz – quartz.

2004). The $\epsilon_{\text{Hf}}(t)$ values were calculated with reference to the chondritic uniform reservoir (CHUR) with present-day $^{176}\text{Hf}/^{177}\text{Hf} = 0.282772$ and $^{176}\text{Lu}/^{177}\text{Hf} = 0.0332$ (Blichert-Toft & Albarede, 1997). The single-stage Hf model ages (T_{DM}) were calculated with reference to depleted mantle with present-day $^{176}\text{Hf}/^{177}\text{Hf} = 0.28325$ and $^{176}\text{Lu}/^{177}\text{Hf} = 0.0384$ (Griffin *et al.* 2000), which can only provide a minimum age for the source material of the magma from which the zircons crystallized. The two-stage model Hf ages (T_{DM2}) were calculated by projecting the initial $^{176}\text{Hf}/^{177}\text{Hf}$ ratios of the zircon back to the depleted mantle model growth curve, which assumes that the parental magma was produced from an average continental crust ($^{176}\text{Lu}/^{177}\text{Hf} = 0.015$) that was originally derived from the depleted mantle (Griffin *et al.* 2002). Thus, two-stage Hf model ages (T_{DM2}) were used in this study. The Lu–Hf isotopic data of the studied samples are provided in online Supplementary Table S6.

4. Analytical results

4.a. Zircon morphology, Th/U ratios and rare Earth elements

In general, the majority of the zircons are colourless and transparent with a varying diameter of 85–259 μm . CL images show that most of the zircon grains have oscillatory or sector/planar zoning. Some zircon grains are euhedral to subhedral in shape, suggesting a limited transportation distance, while most of the zircon grains are rounded to sub-rounded, suggesting long-distance transport and recycled sedimentary processing (Fig. 4).

Previous studies have showed that zircons of igneous and metamorphic origin have different Th/U ratios and trace-element characteristics. Metamorphic zircons are usually found to have a Th/U ratio of < 0.1 and typically negative Eu anomalies, positive Ce anomalies with heavy rare Earth element (HREE) enrichment, that is, high HREE/LREE (light rare Earth element) ratios, whereas magmatic zircons have higher Th/U ratios (mostly 0.2–1.0) and are characterized by a relative depletion of HREEs and flat rare Earth element (REE) patterns without a negative Eu anomaly (Hidaka

et al. 2002; Hoskin & Schaltegger, 2003). However, there are exceptions to this rule; some magmatic zircons have been reported to have a Th/U ratio of < 0.1 and some metamorphic zircons have a Th/U ratio of > 0.1 (Hidaka *et al.* 2002). A comprehensive analysis of internal structures and Th/U ratios, together with REEs, is therefore necessary to investigate zircon origins.

The majority of the zircons in samples P40-01 and P43-01 have a Th/U ratio of > 0.1 , of which 159 grains (93%) have a Th/U ratio of > 0.2 (Fig. 5 and online Supplementary Table S2), indicating that zircons in our samples are largely of igneous origin. A few zircons exhibit sector/planar zonation or bright structureless characters with a Th/U ratio of < 0.1 (Fig. 5), which are interpreted to be of metamorphic origin. Figure 6 shows the chondrite-normalized REE patterns of zircons from these two samples. Most of the zircons have variably high total REE contents (171.33–1820 ppm) showing prominent HREE enrichment with positive Ce anomalies and negative Eu anomalies, typical of igneous origin. Only two zircon grains from the samples do not show negative Eu anomalies; these are interpreted as having formed in plagioclase-absent assemblages, including kimberlite, syenite and eclogite (Belousova *et al.* 2002; Rubatto, 2002; Bingen *et al.* 2004). Four zircons show no positive Ce anomaly but an obvious negative Eu anomaly, suggesting reworking of crustal material, a process that leads to the enrichment of LREEs (Peck *et al.* 2001).

4.b. Zircon U–Pb ages

We determined U–Pb ages of 171 detrital zircon grains from the two sandstone samples (P40-01 and P43-01). Zircons from the two samples have similar age spectra and can therefore be discussed together. The zircon ages vary widely from 532 Ma to 3545 Ma, indicating that they either originated from multiple provenances or from a source with a complex prior history. Nearly all the analysed zircons show $< 10\%$ discordance on the concordia plots (Fig. 7a,c). For sample P40-01, the zircons show age populations of 2047–2566 Ma with a peak at 2463 ± 30 Ma (MSWD = 2.8, $n = 12$), 896–1006 Ma with a peak at 933 ± 7 Ma (MSWD = 3.3,

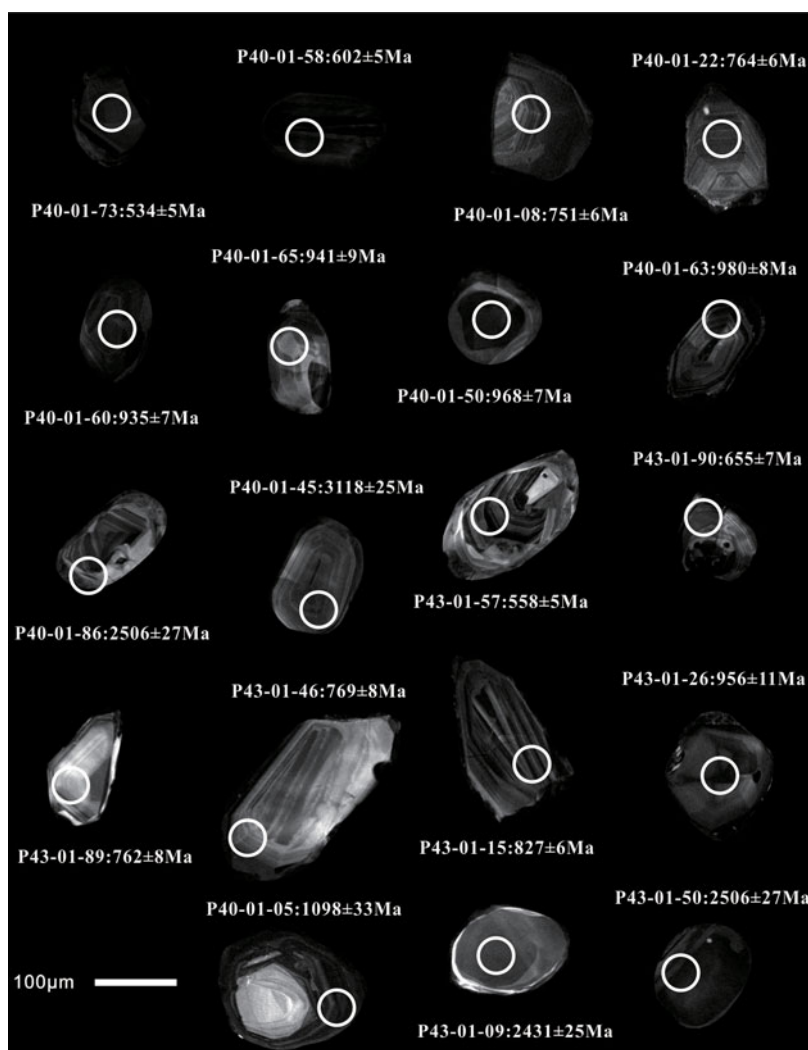


Fig. 4. Representative cathodoluminescence (CL) images of selected detrital zircons with ages and dating spots as indicated.

$n = 20$), 737–870 Ma with a peak at 751 ± 9 Ma (MSWD = 2.4, $n = 7$) and 532–650 Ma with two small peaks at 606 ± 7 Ma (MSWD = 1.0, $n = 2$) and 533 ± 8 Ma (MSWD = 0.042, $n = 2$) (Fig. 7b). Sample P43-01 also shows the same four major age clusters of 2329–2843 Ma with a peak at 2495 ± 24 Ma (MSWD = 1.9, $n = 13$), 890–1002 Ma with a peak at 957 ± 8 Ma (MSWD = 3.3, $n = 17$), 716–866 Ma with a peak at 766 ± 11 Ma (MSWD = 3.9, $n = 10$) and 543–655 Ma with two small peaks at 642 ± 28 Ma (MSWD = 2.8, $n = 3$) and 549 ± 22 Ma (MSWD = 2.5, $n = 3$) (Fig. 7d). According to the youngest concordant age obtained from the sample, which is identical to the maximum depositional age of the sedimentary rock (Sun *et al.* 2008), the timing of deposition of P40-01 and P43-01 was later than 532 ± 8 Ma and 543 ± 6 Ma, respectively.

4.c. Zircon Hf isotopic compositions

Zircon Hf isotopic compositions were analysed for 76 zircon grains which show concordant U–Pb ages from the studied samples. Variations in Hf isotopic ratios $\epsilon_{\text{Hf}}(t)$ with their U–Pb ages are shown in Figure 8. Overall, the late Neoproterozoic and early Cambrian samples plot in a similar position. Zircons of age $c.$ 2.2–2.6 Ga have $\epsilon_{\text{Hf}}(t)$ values of -13.7 to $+4.1$ with model ages

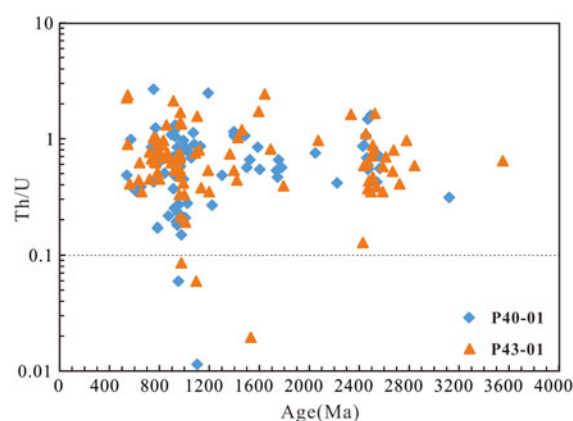


Fig. 5. (Colour online) Age (Ma) versus Th/U ratio of detrital zircons for the late Neoproterozoic – early Cambrian sandstone samples from the Cathaysia Block.

(T_{DM2}) of 2.7–3.4 Ga, indicating the addition of juvenile material and the reworking of Eoarchean–Mesoarchean crustal components. Zircons from the prominent population at $c.$ 0.9–1.0 Ga have $\epsilon_{\text{Hf}}(t)$ values of -11.1 to $+10.2$ with model ages (T_{DM2}) of 1.18–2.50 Ga, suggesting contributions from both juvenile and

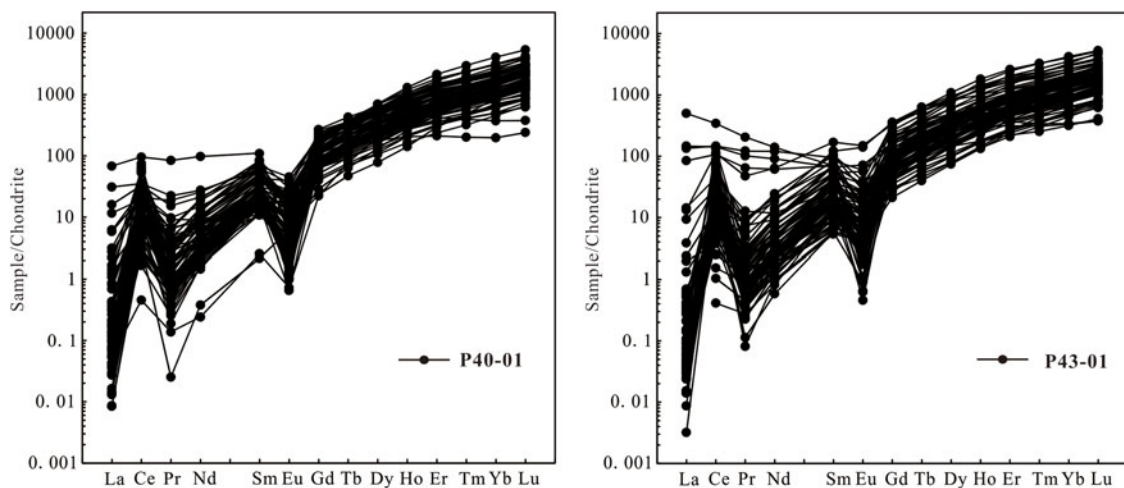


Fig. 6. Chondrite-normalized REE patterns for zircons from sandstone samples (a) P40-01 and (b) P43-01 from the Cathaysia Block. Chondrite REE values used are from Sun & McDonough (1989).

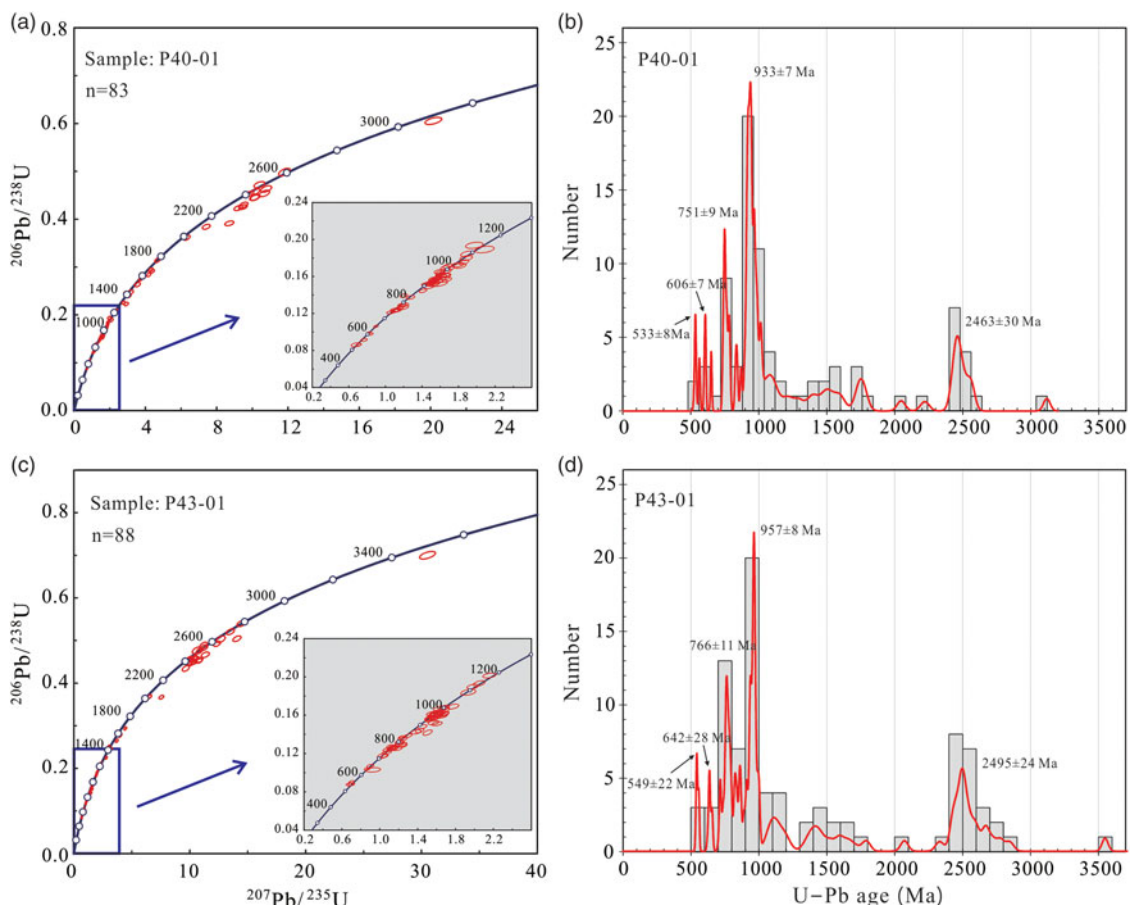


Fig. 7. (Colour online) (a, c) U-Pb Concordia diagrams and (b, d) corresponding frequency distribution of U-Pb ages for detrital zircons from the sandstone samples in the Cathaysia Block.

reworked crustal materials. Zircons with ages of 0.72–0.86 Ga are characterized by negative $\epsilon_{\text{Hf}}(t)$ values that vary from -27.9 to -1.7 with model ages (T_{DM2}) of 1.8–3.4 Ga. The wide range of negative $\epsilon_{\text{Hf}}(t)$ values indicates that these zircons mainly crystallized from reworked Palaeoarchean – early Palaeoproterozoic crust. Zircons from the subordinate population of age *c.* 0.53–0.65 Ga yielded a range of $\epsilon_{\text{Hf}}(t)$ values from -19.4 to $+5.0$ with model

ages (T_{DM2}) of 1.26–1.40 Ga and 1.8–2.7 Ga, indicating remelting of middle Mesoproterozoic juvenile crust and reworking of Neoproterozoic – early Palaeoproterozoic crustal components.

4.d. Whole-rock geochemistry

The major- and trace-element analyses are provided in online Supplementary Table S1 (available at <http://journals.cambridge>).

org/geo). In terms of major elemental compositions, the studied samples of late Neoproterozoic and early Cambrian age are on the whole characterized by intermediate to high SiO_2 (47.2–78.0 wt%), and relatively high Al_2O_3 (9.1–24.8 wt%) and $\text{Fe}_2\text{O}_3^{\text{T}} + \text{MgO}$ (5.6–11.8 wt%, average 8.2 wt%) (where $\text{Fe}_2\text{O}_3^{\text{T}}$ represents total FeO content). They all have low CaO content (typically < 1 wt%). In addition, there are obvious negative correlations of SiO_2 with TiO_2 ($r = -0.88$), Al_2O_3 ($r = -0.98$), $\text{Fe}_2\text{O}_3^{\text{T}}$ ($r = -0.70$), MgO ($r = -0.91$) and K_2O ($r = -0.94$), as shown in Figure 9.

The trace-element concentrations are also highly variable with large-ion lithophile elements (LILEs) such as Rb, Ba, Th and U having relatively higher content than the value of the post-Archean Australian shale (PAAS; Taylor & McLennan, 1985). The high-field-strength elements (HFSEs) such as Zr, Hf and Y are also enriched in these samples, but variably depleted in Nb and Ta relative to the PAAS. In addition, all the samples show similar chondrite-normalized REE patterns with a significant LREE enrichment and relatively flat HREE distribution (Fig. 10), with varying La/Sm_N (3.01–5.22), Gd/Yb_N (1.28–2.10) and La/Yb_N (7.35–14.43) ratios and distinctive negative Eu anomalies (Eu/Eu* = 0.45–0.65). Although the absolute concentrations of REEs vary, the overall chondrite-normalized patterns of the samples resemble those of the average PAAS (McLennan, 1989) and upper continental crust (Rudnick & Gao, 2003), suggesting that the sedimentary rocks were derived from an upper crustal source.

5. Discussion

5.a. Source-rock geochemical constraints

5.a.1. Source area weathering

Palaeoweathering in the source area is among the most important processes affecting the chemical compositions of sedimentary rocks (Nesbitt & Young, 1982; McLennan *et al.* 1993; Fedo *et al.* 1995). The chemical index of alteration (CIA) is a frequently used parameter to quantify the degree of source area weathering ($\text{CIA} = [\text{Al}_2\text{O}_3 / (\text{Al}_2\text{O}_3 + \text{CaO}^* + \text{Na}_2\text{O} + \text{K}_2\text{O})] \times 100$; Nesbitt & Young, 1982; McLennan *et al.* 1993). The pre-metasomatized CIA values of the sandstones in our study range from 56 to 84 (Fig. 11), indicating moderate weathering conditions in the source area. By employing the CIA values in the $\text{Al}_2\text{O}_3 - \text{CaO} + \text{Na}_2\text{O} - \text{K}_2\text{O}$ (A-CN-K) ternary diagram, one can more effectively evaluate the weathering degree (Nesbitt & Young, 1982; Fedo *et al.* 1995). In the absence of post-depositional K metasomatism, the ideal weathering path would be a linear trend parallel to the A-CN side (Fig. 11). In contrast, the sandstones that have undergone K-metasomatism would deviate towards the A-K boundary and have smaller CIA values (Rainbird *et al.* 1990; Fedo *et al.* 1995). The majority of the studied samples are nearly parallel to the predicted weathering trend, illustrating the limited influence of K-metasomatism on these samples. Several samples plot to the A-K boundary and exhibit CIA values lower than the pre-metasomatized trend, indicating moderate post-depositional K-metasomatism (Fig. 11).

The plagioclase index of alteration (PIA) is another parameter to quantify the degree of chemical weathering that can eliminate the influence of K-metasomatism ($\text{PIA} = [(\text{Al}_2\text{O}_3 - \text{K}_2\text{O}) / (\text{Al}_2\text{O}_3 + \text{CaO}^* + \text{Na}_2\text{O} - \text{K}_2\text{O})] \times 100$; Fedo *et al.* 1995). The PIA values (49–96, average 76) of the studied samples are relatively higher than CIA values, confirming a moderate degree of weathering. Sedimentary recycling under oxidizing conditions usually results in fractionation of Th and U because of the oxidation

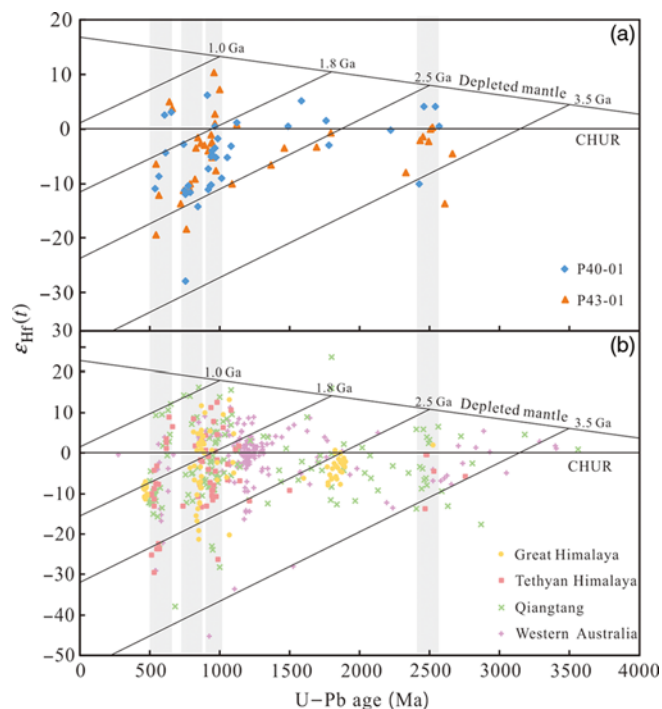


Fig. 8. (Colour online) $\epsilon_{\text{Hf}}(t)$ versus U–Pb ages of the detrital zircons from the studied sandstone samples in the Cathaysia Block. CHUR – chondritic uniform reservoir. The declining parallel lines are two-stage Hf model ages (T_{DM2}). The detrital zircon data from the Greater Himalaya (Spencer *et al.* 2012), Tethyan Himalaya (Zhu *et al.* 2011), Qiangtang (Dong *et al.* 2011; Zhu *et al.* 2011) and Western Australia (Veevers *et al.* 2005) are shown for comparison.

and loss of uranium during weathering (McLennan & Taylor, 1980). Thus, the Th/U ratios of sedimentary rocks increase during successive cycles of weathering and redeposition (Taylor & McLennan, 1985). The Th/U ratios in our study (4.01–7.07, average 5.6) are typically higher than the average value for the upper crust (3.8; McLennan & Taylor, 1980), providing additional support for a moderate weathering history in the source area.

5.a.2. Source-rock composition

The geochemical characteristics of the sedimentary rocks can also provide useful information to elucidate the sedimentary provenance and composition of the crustal source regions (Bhatia, 1983; Bhatia & Crook, 1986; Roser & Korsch, 1986; Floyd & Leveridge, 1987; Gu *et al.* 2002). Before using the immobile elements to identify the possible source rocks, it is necessary to evaluate their relative mobility during erosion, transportation and sedimentation (Singh, 2009). Immobile elements hosted in common minerals will have similar hydrodynamic behaviours and show a linear array of coordinates pointing to the origin, whereas chemically mobile elements will show a large deviation (Fralick & Kronberg, 1997). Most of the samples show general positive correlations in the plots of $\text{Fe}_2\text{O}_3^{\text{T}}$ versus Al_2O_3 , TiO_2 versus Al_2O_3 and TiO_2 versus $\text{Fe}_2\text{O}_3^{\text{T}}$ (Fig. 12), indicating that the aforementioned elements have remained chemically immobile and have been affected by sorting in a similar manner (Fralick & Kronberg, 1997; Singh, 2009; Wang *et al.* 2018). The linear arrangement of TiO_2 , Al_2O_3 and $\text{Fe}_2\text{O}_3^{\text{T}}$ extend towards 100% SiO_2 , also suggesting they are chemically immobile and enriched in the fine fractions (Fig. 9; Fralick & Kronberg, 1997). The aforementioned immobile element ratios should therefore represent the average

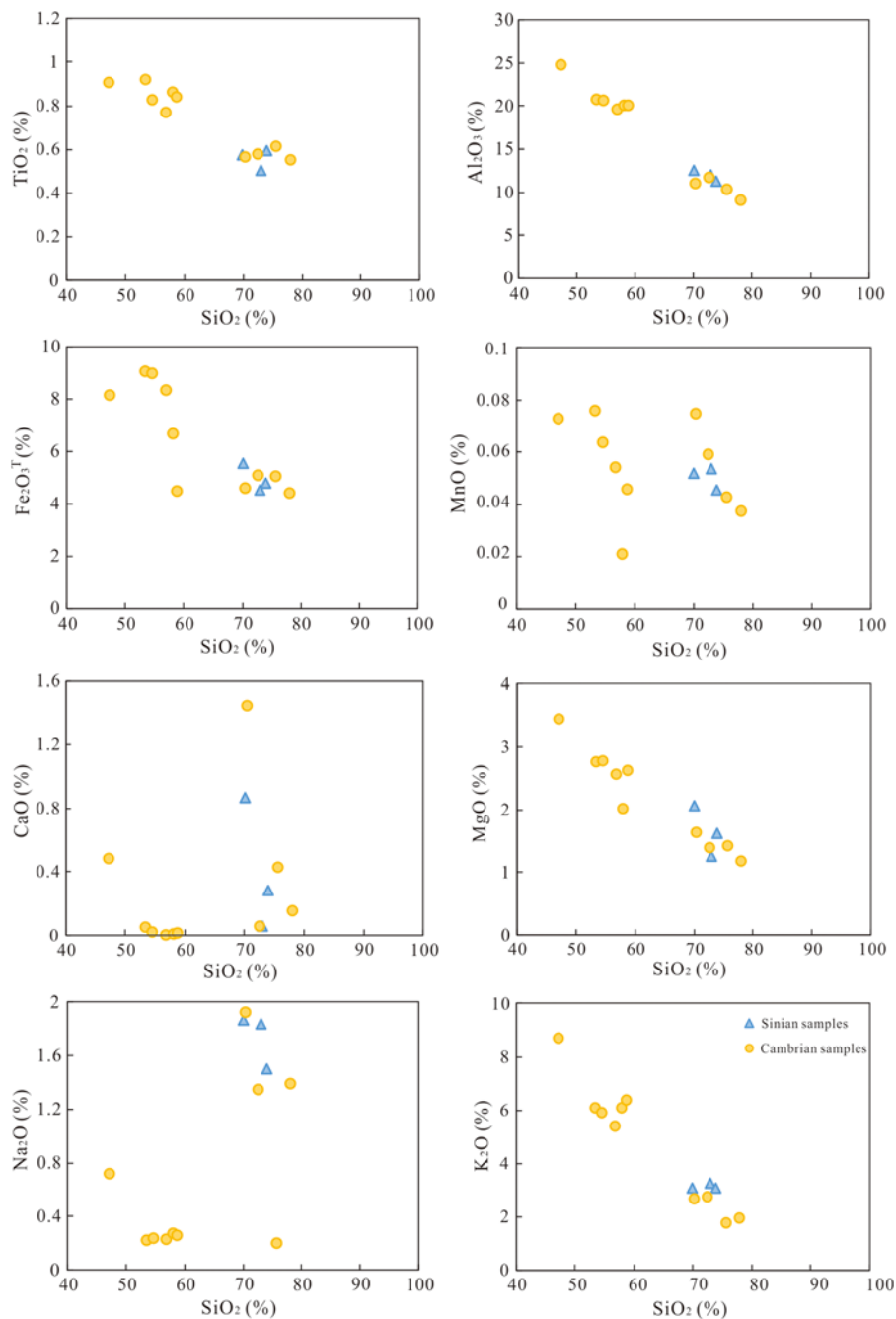


Fig. 9. (Colour online) Variation diagrams of major elements versus SiO_2 (%) for the studied sedimentary rocks from late Neoproterozoic and early Cambrian time. Note the negative correlations for SiO_2 versus TiO_2 , Al_2O_3 , Fe_2O_3^T , MgO and K_2O .

ratio of their source rocks. In the plots of $\text{Fe}_2\text{O}_3^T/\text{Al}_2\text{O}_3$ and $\text{TiO}_2/\text{Fe}_2\text{O}_3^T$ versus $\text{TiO}_2/\text{Al}_2\text{O}_3$ (Fig. 13) the samples cluster between the average composition of felsic volcanic rock, TTG, andesite and granite but far from the basaltic compositions, suggesting that the source was mainly composed of felsic to intermediate components. In addition, constraint for the initial composition of the source rocks can also be obtained from the A-CN-K diagram (Nesbitt & Young, 1982; Fedo *et al.* 1995). All the studied samples plotted in the area between the weathering trends of granodiorite and granite (Fig. 11), further indicating that the source rocks were possibly a mixture of intermediate to felsic igneous rocks.

Trace elements with relatively low mobility and low residence time in seawater are quantitatively transferred into clastic sediments during primary weathering and transportation, and can therefore be used to identify the composition of source rocks (Bhatia & Crook, 1986; Floyd & Leveridge, 1987; Floyd *et al.* 1989; McLennan, 1989). The concentrations of Th and La are more enriched in felsic than in mafic igneous source rocks, whereas the Co, Sc and Cr abundances are higher in mafic rocks (Taylor & McLennan, 1985). In the present study, the samples show a relatively high La/Sc (4.0) ratio with low Sc/Th (0.68), Cr/Th (3.97) and Co/Th (4.5) ratios, indicating the rocks were most likely derived

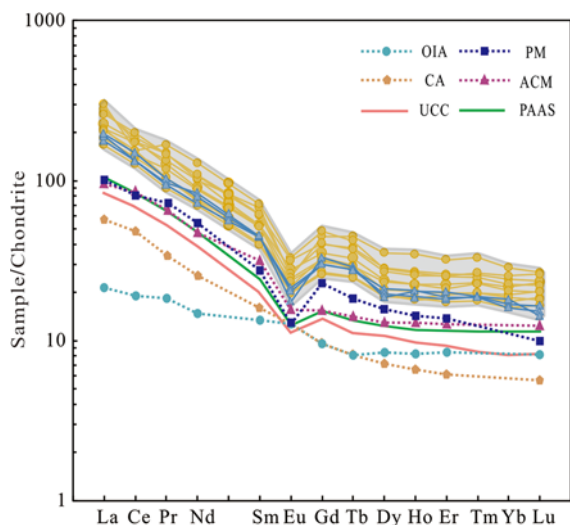


Fig. 10. (Colour online) Chondrite normalized rare Earth element patterns for the late Neoproterozoic – early Cambrian sedimentary rocks in the Cathaysia Block, normalized to chondritic values from Sun & McDonough (1989). The standard composition of average post-Archean Australian shale (PAAS) after McLennan (1989) and upper continental crust (UCC) after Rudnick & Gao (2003) are shown for comparison; various tectonic conditions data after Bhatia (1986). OIC – oceanic island arc; CA – continental arc; ACM – active continental margin; PM – passive margin. Symbols as for Figure 9.

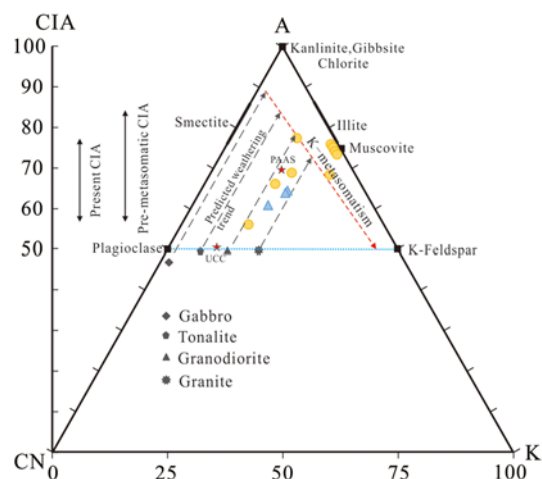


Fig. 11. (Colour online) A-C-N ternary diagram (in molecular proportions) (after Nesbitt & Young, 1982; Fedo *et al.* 1995). Average gabbro, tonalite, granodiorite, granite, UCC and PAAS data are from Condie (1993). Arrows represent the separately predicted weathering trends of gabbro, tonalite, granodiorite and granite. Symbols as for Figure 9.

from a felsic source rock (Table 1). Some other compositional discrimination diagrams also can distinguish the compositional characteristics of the source rocks. According to the discrimination diagram of the La/Th ratio versus Hf (Fig. 14a), most samples fall in the field of a felsic source with a minor old sedimentary component. The Co/Th versus La/Sc ratios plot (Fig. 14b) shows a mixed source, dominated by felsic–intermediate materials. In the plot of TiO₂ versus Ni (Fig. 14c), the majority of samples fall in the acidic magmatite field. As shown in the (La/Yb)_n versus Eu/Eu* plot (Fig. 14d), all the samples indicate contributions from felsic to intermediate components. These features all indicate that the studied late Neoproterozoic and early Cambrian sandstones were derived from a source dominated by felsic–intermediate materials.

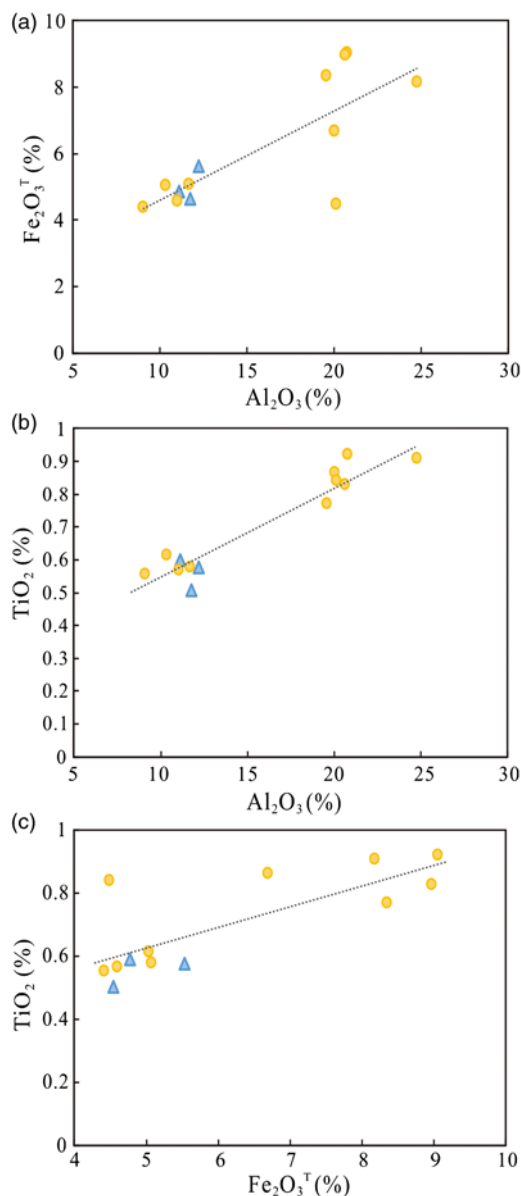


Fig. 12. (Colour online) (a–c) Plots of sedimentary rocks in the bivariate diagrams between different elements. Positive correlations in these binary diagrams demonstrate that the elements Fe, Ti and Al were chemically immobile and have similar geochemical behaviour during sedimentation. Symbols as for Figure 9.

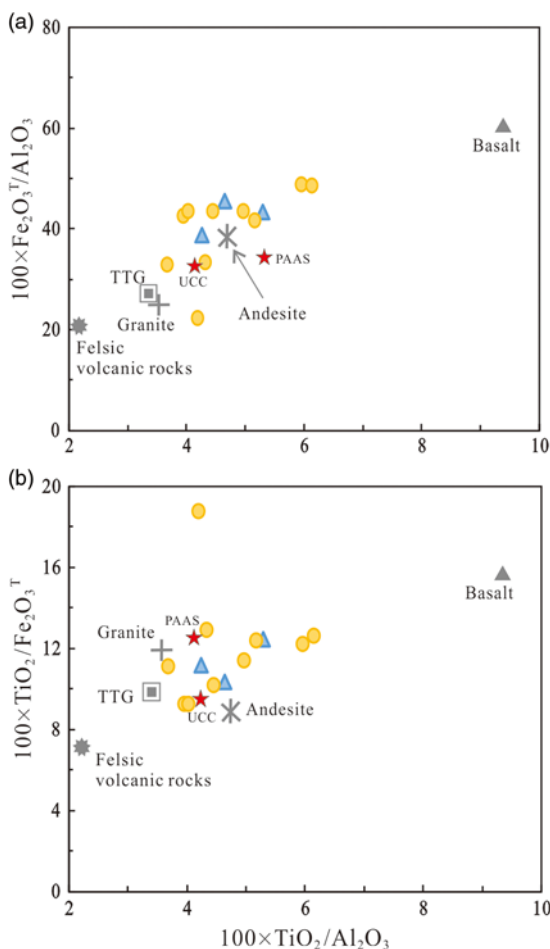
5.b. Provenance of the detrital zircons

The age distribution of the detrital zircons can be used to trace the provenance of the sedimentary rocks (Fedo *et al.* 2003). The similar age spectra of the late Neoproterozoic and early Cambrian samples indicate a continuous sedimentary process and can therefore be discussed together. The zircon U–Pb ages obtained from the Cathaysia Block in this study defined four major age populations as follows: 2221–2676 Ma (with a peak of 2500 Ma), 900–1000 Ma (with a peak of 966 Ma), 716–870 Ma (with a peak of 752 Ma) and 532–655 Ma (with two peaks at 536 and 604 Ma) (Fig. 15a).

The oldest populations of zircons in our samples range from 2221 Ma to 3545 Ma with a peak at *c.* 2.5 Ga, broadly corresponding to the timing of a global crustal growth event (Santosh *et al.* 2013). Although similar ages have been widely reported from detrital or inherited grains or xenocrysts in Proterozoic–Mesozoic

Table 1. Elemental ratios of the late Neoproterozoic – early Cambrian sedimentary rocks in this study compared with ratios from other sources

Lithology	La/Sc	Sc/Th	Cr/Th	Co/Th	Data source
Sediments from mafic sources	0.4–1.1	20–25	22–100	7.1–8.3	Cullers, 1994
Sediments from felsic sources	2.5–16	0.05–1.2	0.5–7.7	0.22–1.5	Cullers, 1994
Upper continental crust	2.7	1	3.3	0.9	Taylor & McLennan, 1985
Lower continental crust	0.3	34	222	33	Taylor & McLennan, 1985
Sandstones	4.00	0.68	3.97	0.45	This study

**Fig. 13.** (Colour online) Source-rock discrimination diagrams for the sedimentary rocks plotted as (a) $100 \times \text{TiO}_2/\text{Al}_2\text{O}_3$ versus $100 \times \text{Fe}_2\text{O}_3/\text{Al}_2\text{O}_3$ and (b) $100 \times \text{TiO}_2/\text{Fe}_2\text{O}_3$ versus $100 \times \text{TiO}_2/\text{Al}_2\text{O}_3$. Average Proterozoic felsic volcanic rocks, granite, TTG, andesite, basalt, UCC and PAAS data are from Condie (1993) for comparison. Symbols as for Figure 9.

igneous/sedimentary rocks from the Cathaysia Block, rocks of these ages are rarely exposed at present (Xu *et al.* 2005, 2007; Wang *et al.* 2010; Xia *et al.* 2012). The Archean basement in the SCB has only been found in the northern part of the Yangtze Block, represented by the Kongling Complex. The detrital zircon age spectra for this complex is quite different and cannot be the

provenance for the Neoproterozoic–Cambrian sedimentary rocks we studied (Fig. 15a,c). Furthermore, most of these zircons are highly rounded (Fig. 4), suggesting long-distance transport from their source region or multi-cycled histories before their deposition. Because of the few coeval magmatic rocks of age *c.* 2.5 Ga known from the SCB, it is reasonable to conclude that these zircons were likely derived from an exotic source that was once contiguous to the SCB. This conclusion is also supported by the Hf isotopic compositions of the detrital zircons. Most Neoproterozoic zircons from the studied samples show similar values to those of India, Qiangtang and east Antarctica, but different from those in Western Australia, which underwent a major period of granitoid production at the older ages of 2.6–2.8 Ga (Fig. 8b; Zhu *et al.* 2011). The detrital zircons of age *c.* 2.5 Ga in the Cathaysia Block could potentially have come from India, Qiangtang and east Antarctica.

A prominent age population (900–1000 Ma) with a peak at 966 Ma has been found in the Cathaysia Block, corresponding to the global Grenvillian Orogeny associated with the amalgamation of Rodinia (Fig. 15a,b; Zhao & Cawood, 2012). Detrital zircons of this age are reported to be widespread in SCB sedimentary rocks, although the exposure of Grenvillian rocks is limited (Fig. 15a–c; Yu *et al.* 2008; Shu *et al.* 2011). Similarly aged magmatic rocks in the Cathaysia Block are the 0.97 Ga Jingnan rhyolites in the southwestern Wuyi Mountains and the 0.91–1.0 Ga metabasites in the northern Yunkai Domain (Shu *et al.* 2008; Xia *et al.* 2015). Subduction-related magmatic rocks with ages of *c.* 0.9–1.0 Ga of arc-continent origin have been reported in the eastern and southeastern margin of the Yangtze Block (Ye *et al.* 2007; Xia *et al.* 2018). Several mafic rocks with ages of 0.98–1.1 Ga have also been found in the northern margin of the Yangtze Block (Peng *et al.* 2012). However, it is noteworthy that most of the reported rocks of these ages in the SCB are dominated by metamorphic rocks or mafic intrusions (Xia *et al.* 2015, 2018). Given the aforementioned felsic source characteristic of our samples and the moderately to highly rounded zircon morphology, this should preclude the possibility of a local source supply for the voluminous early Neoproterozoic zircons in our study. The age spectra of the known Cathaysia crystalline basement rocks lacking an age population at 0.9–1.0 Ga also suggest an unlikely source from the recycling of underlying strata (Fig. 15a,b). Moreover, the nearly entire water coverage of the Cathaysia Block with continuous NW palaeocurrents across Cathaysia to the Yangtze Block during early Palaeozoic time suggests an outboard source should lie to the SE margin of the Cathaysia Block (Wang *et al.* 2010; Xu *et al.* 2013; Shu *et al.* 2014; Yao *et al.* 2015). Furthermore, the 0.9–1.0 Ga detrital zircons with a wide range of $\epsilon_{\text{Hf}}(t)$ values (–11.1 to +10.2) and model ages (1.17–2.50 Ga) may suggest a common provenance with that in the Himalaya regions of India and Qiangtang (Fig. 8a,b). This age population matches well with the recorded synchronous arcs in the Eastern Ghats belt (960 Ma) of India and the Prince Charles Mountains (960–990 Ma) of East Antarctica during the assembly of the Rodinia supercontinent (Fitzsimons, 2000a, b; Veevers, 2007), but is much younger than the pronounced *c.* 1100–1300 Ma Grenvillian Event in other blocks such as Western Australia and West Laurentia, indicating the diachronic nature of the Rodinia assembly process (Li *et al.* 2014). The large proportion of early Neoproterozoic zircons (0.9–1.0 Ga) therefore indicates a possible source from the Eastern Ghats belt in India or the Prince Charles Mountains in East Antarctica.

The detrital zircons also show another cluster of middle Neoproterozoic ages (716–870 Ma, a peak at 752 Ma) corresponding to the break-up of the Rodinia supercontinent (Shu *et al.* 2011;

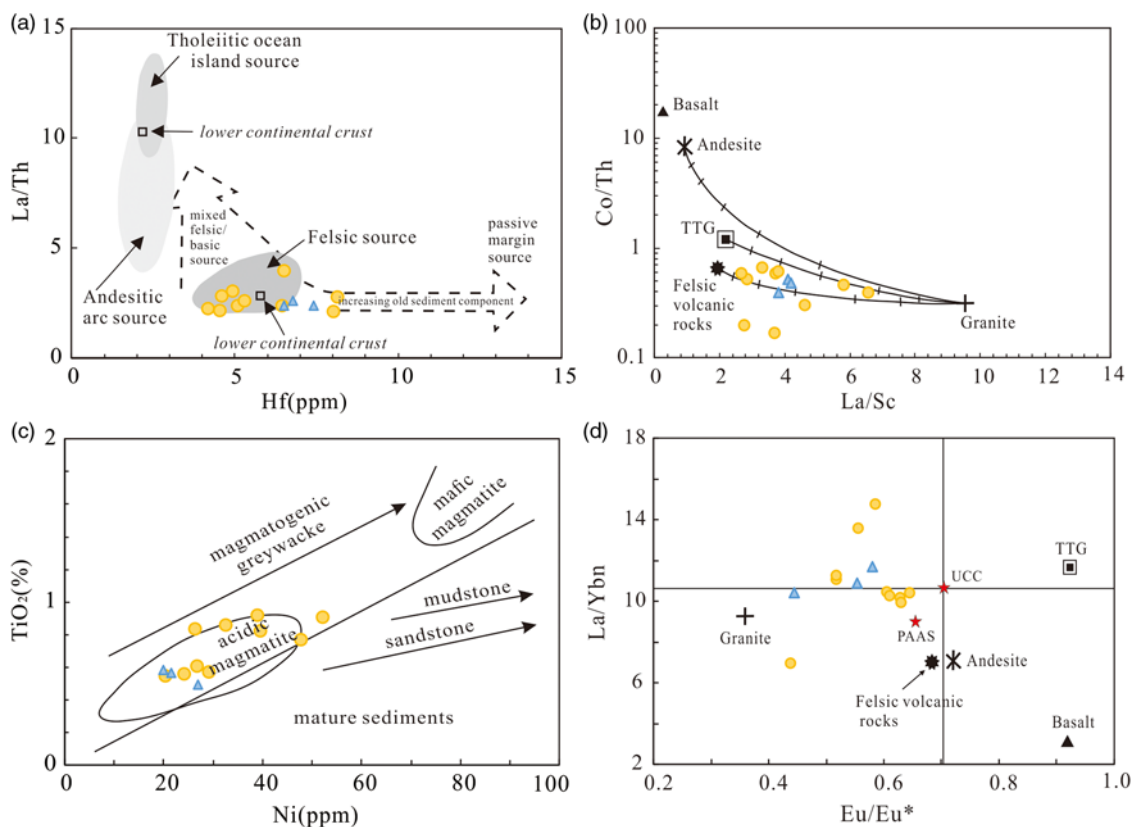


Fig. 14. (Colour online) Geochemical diagrams showing the source composition of late Neoproterozoic – early Cambrian sedimentary rocks in the Cathaysia Block. (a) La/Th versus Hf (after Floyd & Leveridge, 1987); (b) Co/Th versus La/Sc (after Gu *et al.* 2002); (c) TiO₂ versus Ni (after Floyd *et al.* 1989); and (d) (La/Yb)_n versus Eu/Eu* (after Wang *et al.* 2018). Average reference compositions are from Condie (1993). Symbols as for Figure 9.

Li *et al.* 2014). The Panxi–Hannan Belt along the western margin of the Yangtze Block contains voluminous 730–870 Ma mafic to intermediate igneous intrusions (Zhao & Cawood, 2012; Xia *et al.* 2018). However, the dominant carbonate deposition over the Yangtze Block makes it an unlikely source for the clastic sediments in the Cathaysia Block (Xu *et al.* 2013; Shu *et al.* 2014; Yao *et al.* 2014, 2015). Rift-related magmatic assemblies, S-type granites and collision-rifting tectonic processes during this period have been widely reported in the Yangtze Block but are quite limited in the Cathaysia Block (Yao *et al.* 2011, 2014; Wang *et al.* 2013; Xia *et al.* 2018). Similar detrital age populations have also been well documented in the middle Neoproterozoic successions of the Nanhua Basin (635–850 Ma) (Wang *et al.* 2012). In addition, all the zircons with these ages yield negative $\epsilon_{\text{Hf}}(t)$ values (–1.7 to –27.9) and the model ages are mainly clustered at 1.84–1.96 Ga and 2.3–2.8 Ga (Fig. 8a), consistent with values from the Neoproterozoic igneous zircons in the central Nanhua Basin (Wang *et al.* 2012; Zhang & Zheng, 2013). Combined with the mostly euhedral to subeuhedral zircon morphology, one can infer that these zircons derived from a mainly local supply within the SCB and were most probably sourced from the elevated rift shoulders and rifting volcanic rocks of the Nanhua Basin.

Some of the zircons with an age range of 532–655 Ma (two peaks at 536 Ma and 604 Ma) deserve attention. They possibly correspond to the timing of the global Pan-African Event related to the assembly of the Gondwana supercontinent, and the 530 Ma peak may be interpreted as the final assembly of Gondwana (Cawood & Nemchin, 2000; Shabeer *et al.* 2005). Although no

coeval magmatic or metamorphic rocks have been found in the SCB during this period, the reported detrital zircons of similar ages from the Neoproterozoic to Cambrian sedimentary rocks of the Cathaysia and Yangtze blocks indicate that a provenance should exist for these detrital zircons (Fig. 15a,b,c). In contrast, this age population is comparable to the timing of the East African Orogen (650–550 Ma) related to the subduction of oceanic floor between cratons (DeCelles *et al.* 2000; Duan *et al.* 2011), the Bhimphedian Orogen (550–470 Ma) associated with the proto-Tethyan oceanic subduction beneath the margins of the Gondwana continents (Cawood *et al.* 2007) and the Prydz–Darling Orogen (600–500 Ma) between India and the Antarctic (Cawood *et al.* 2007). The Hf isotopic compositions of the zircons of these ages show a special variation, in that the zircons of age > 570 Ma show either positive or negative $\epsilon_{\text{Hf}}(t)$ values, whereas the $\epsilon_{\text{Hf}}(t)$ values of the zircons of age < 570 Ma zircons are exclusively negative (Fig. 8a). It was inferred that the source regions of these zircons underwent juvenile input during the period 650–570 Ma but more intense reworking of ancient crustal materials during the period 570–530 Ma. These zircon Hf isotopic characteristics are consistent with those in the Himalaya regions of India and Qiangtang, including the commonly positive $\epsilon_{\text{Hf}}(t)$ values at *c.* 650–570 Ma (Fig. 8a,b). Moreover, the palaeocurrent records in the Neoproterozoic – early Palaeozoic sedimentary rocks from East Gondwana could have led to widespread detritus transport into the SCB (Myrow *et al.* 2006, 2010). The commonly rounded to sub-rounded zircons of our samples may therefore have derived from East Gondwana, and most probably from the East African and Bhimphedian orogens.

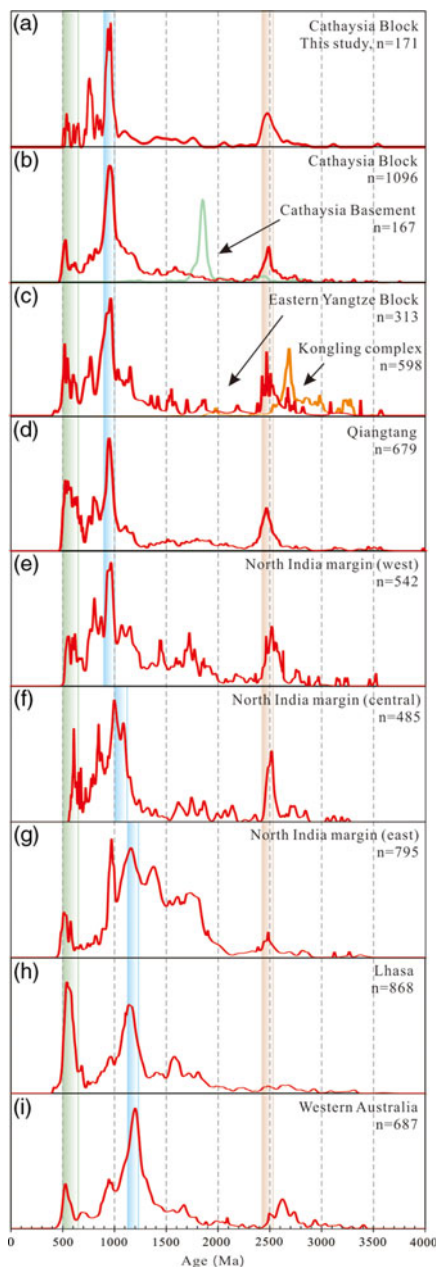


Fig. 15. (Colour online) (a–i) Relative probability diagrams of U–Pb detrital zircon age distributions for comparing age-equivalent sedimentary samples from the Cathaysia Block with other blocks, including Cathaysia, Yangtze, Qiangtang, northern India margin, Lhasa Terrane and Western Australia. Data from: this study, Yu *et al.* (2008), Wu *et al.* (2010), Yao *et al.* (2014) and Yan *et al.* (2015) for Neoproterozoic–Cambrian sediments in the Cathaysia Block; Li (1997), Wan *et al.* (2007), Liu *et al.* (2009), Yu *et al.* (2009) and Li *et al.* (2010) Wan *et al.* (2007), Liu *et al.* (2009), Yu *et al.* (2009) for the Precambrian crystalline basement rocks in Cathaysia Block; Wang *et al.* (2010) and Yao *et al.* (2015) for Cambrian sediments in the Eastern Yangtze Block; Gao *et al.* (2011) and Guo *et al.* (2014) for the Kongling Complex; Dong *et al.* (2011), He *et al.* (2011), Pullen *et al.* (2011) and Zhu *et al.* (2011) for late Neoproterozoic – early Palaeozoic sediments in the Qiangtang; Myrow *et al.* (2010) and Webb *et al.* (2011) for late Neoproterozoic – early Palaeozoic sediments in the west of the northern India margin; Gehrels *et al.* (2011) for early Palaeozoic sediments in the central part of the northern India margin; McQuarrie *et al.* (2008), Myrow *et al.* (2010), Webb *et al.* (2013) and Guo *et al.* (2017) for late Neoproterozoic – early Palaeozoic sediments in the east of the northern India margin; Leier *et al.* (2007), Dong *et al.* (2010), Zhu *et al.* (2011) and Guo *et al.* (2017) for late Neoproterozoic – Palaeozoic sediments in the Lhasa Terrane; and Cawood & Nemchin (2000), Veevers *et al.* (2005) and Martin *et al.* (2017) for late Neoproterozoic – Palaeozoic sediments in Western Australia.

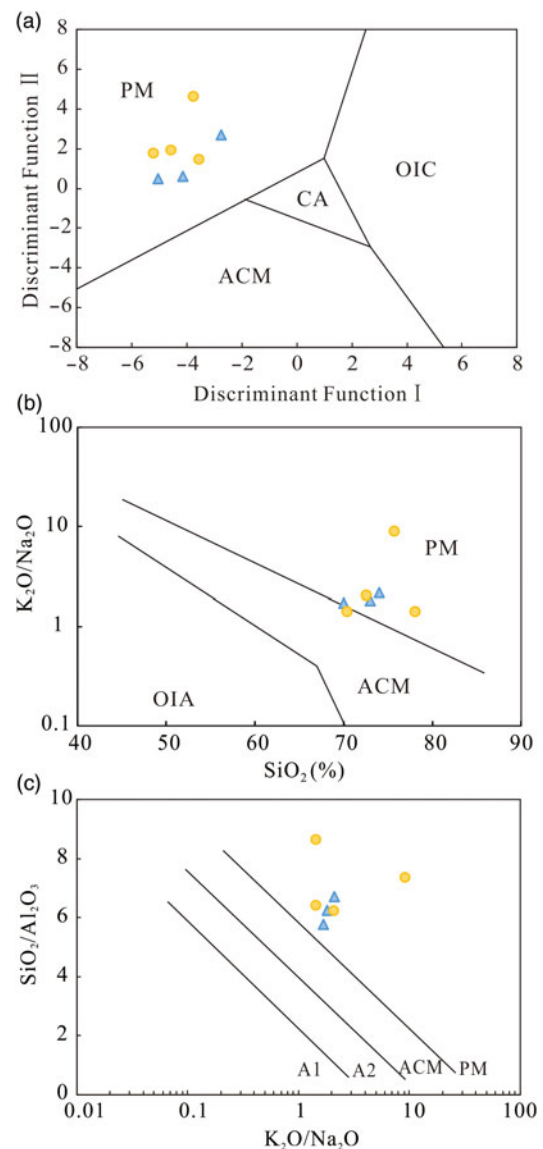


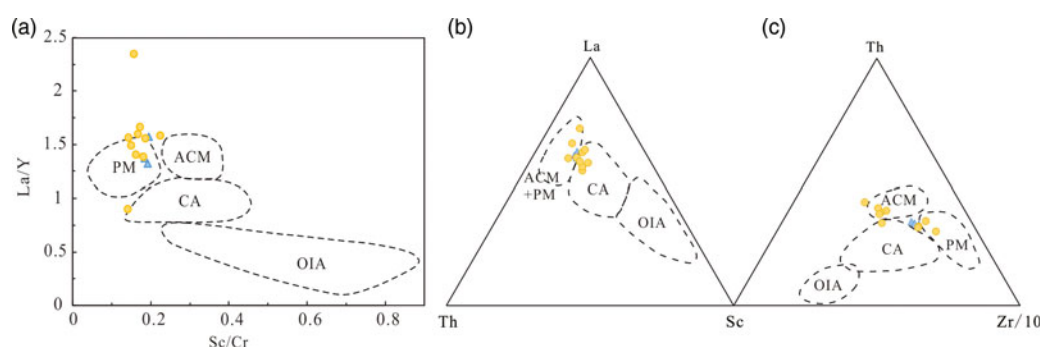
Fig. 16. (Colour online) Tectonic setting discrimination diagram for sedimentary rocks. (a) Discriminant function plot (Bhatia, 1983), (b) SiO_2 versus $\text{K}_2\text{O}/\text{Na}_2\text{O}$ discrimination plot and (c) $\text{SiO}_2/\text{Al}_2\text{O}_3$ versus $\text{K}_2\text{O}/\text{Na}_2\text{O}$ discrimination plot (Roser & Korsch, 1986). OIC – oceanic island arc; CA – continental arc; ACM – active continental margin; PM – passive margin; A1 – island arc of basaltic and andesitic detritus; A2 – evolved island arc of felsic intrusive rock detritus. Symbols as for Figure 9.

5.c. Tectonic implications

The geochemical compositions of sedimentary rocks prove to be useful in characterizing the tectonic setting of sedimentary deposition, and various major- and trace-element discriminants and diagrams have been constructed to identify them (Bhatia, 1983; Bhatia & Crook, 1986; Roser & Korsch, 1986). Four typical tectonic settings are generally distinguished as follows: oceanic island arc (OIA), continental arc (CA), active continental margin (ACM) and passive margin (PM). However, the tectonic discrimination diagrams with major elements must be used with caution because K, Na and Al are relatively mobile during post-depositional processes (Concepcion *et al.* 2012). Based on the A–CN–K ternary diagram (Fig. 11), six sandstone samples underwent moderate post-depositional K-metasomatism; these samples were therefore

Table 2. REE characteristics (ppm) of the late Neoproterozoic – early Cambrian sedimentary rocks in this study for discrimination of tectonic setting. Source: Bhatia (1983).

Element	Oceanic island arc	Andean type continental margin	Continental arc	Passive margin	This study
La	8.0 ± 1.7	37	27.0 ± 4.5	39	52.32
Ce	19.0 ± 3.7	78	59.0 ± 8.2	85	95.85
REE	58 ± 10	186	146 ± 20	210	235.14
La/Yb	4.2 ± 1.3	12.5	11.0 ± 3.6	15.9	15.25
(La/Yb) _N	2.8 ± 0.9	8.5	7.5 ± 2.5	10.8	10.94
Σ _{LREE} /Σ _{HREE}	3.8 ± 0.9	9.1	7.7 ± 1.7	8.5	9.03
Eu/Eu*	1.04 ± 0.11	0.6	0.79 ± 0.13	0.56	0.56

**Fig. 17.** (Colour online) Trace-element tectonic discriminating diagrams for sedimentary rocks (after Bhatia & Crook, 1986). OIC – oceanic island arc; CA – continental arc; ACM – active continental margin; PM – passive margin. Symbols as for Figure 9.

excluded in the tectonic discrimination diagrams using major elements. In the discriminant function plot of 11 major elements of Bhatia (1983), all of the samples lie within the passive continental margin environment (Fig. 16a). This is consistent with the discrimination diagrams of the K_2O/Na_2O ratio versus SiO_2 and SiO_2/Al_2O_3 versus K_2O/Na_2O ratios, which also indicate a passive continental margin tectonic setting (Fig. 16b,c; Roser & Korsch, 1986). On the La/Y versus Sc/Cr ratio discrimination diagram, nearly all the samples fall in the field of passive margin or cluster near the field (Fig. 17a; Bhatia & Crook, 1986). On the ternary diagrams of La-Th-Sc and Th-Sc-Zr/10 (Fig. 17b,c), the samples mostly fall within the fields of passive margin, active continental margin and continental arc, showing somewhat of a difference from the prior discriminations. This inconsistency in using trace elements can be attributed to the inherited geochemical signatures from rocks generated at an ancient active continental margin or continental arc, rather than its depositional environment (Savoy *et al.* 2000; Bai *et al.* 2007; Concepcion *et al.* 2012). This is supported by previous work on the tectonic evolution of the SCB (Shu *et al.* 2011; Yao *et al.* 2011, 2014; Zhao & Cawood, 2012). Moreover, the chondrite-normalized REE patterns of the sandstones containing the most sensitive tectonic discriminant parameters further support a passive margin setting. They show LREE enrichment with significant negative Eu anomalies, which is distinct from the patterns in a continental arc or active continental margin setting (Fig. 10 and Table 2; Bhatia, 1986). U–Pb detrital zircon dating can be used as additional evidence for inferring the tectonic setting of sedimentary rocks (Cawood *et al.* 2012; Wang *et al.* 2018). The ages of detrital zircons in our

study are dominated by the early Neoproterozoic, much older than the depositional age (Sinian or Cambrian), also supporting a passive margin setting (Fig. 18). All these data strongly indicate that the studied sandstones were chiefly deposited in a passive continental margin.

In addition, the tectonic regime between the Cathaysia and Yangtze blocks during early Palaeozoic time remains under debate. Among the issues is whether there was a palaeo-ocean basin (Huanan Ocean) that separated the Cathaysia and Yangtze blocks during Cambrian time (Shui, 1987; Liu & Xu, 1994; Xu *et al.* 1996; Charvet *et al.* 2010; Wang *et al.* 2010; Yao *et al.* 2015). Provenance analysis using U–Pb geochronology can be used to determine this. If the Huanan Ocean existed during Cambrian time, the provenance of the detrital zircons in the sedimentary rocks between the Cathaysia and Yangtze blocks should be different. Here we used the detrital zircon age data from the Cambrian sedimentary rocks between the Cathaysia and Yangtze blocks to test this scenario. Geologically, the two sample sites are SE of the JSF in the western Cathaysia Block (Fig. 1b). The detrital zircon age spectra show major Neoproterozoic age peaks at 1000–900 Ma and 870–716 Ma, along with subordinate late Archean and early Neoproterozoic peaks at c. 2500 Ma and 655–532 Ma, respectively (Fig. 15a). The Cambrian sandstone samples from the Eastern Yangtze Block show the same age spectra with five peaks at 1006–892, c. 778, c. 612, c. 526 and c. 2476 Ma (Fig. 15c; Wang *et al.* 2010; Yao *et al.* 2015). This indicates the sediments in the two blocks derived from a similar provenance across the JSF, arguing against the existence of the Huanan Ocean during the Cambrian. Furthermore, palaeocurrent measurements show a consistent

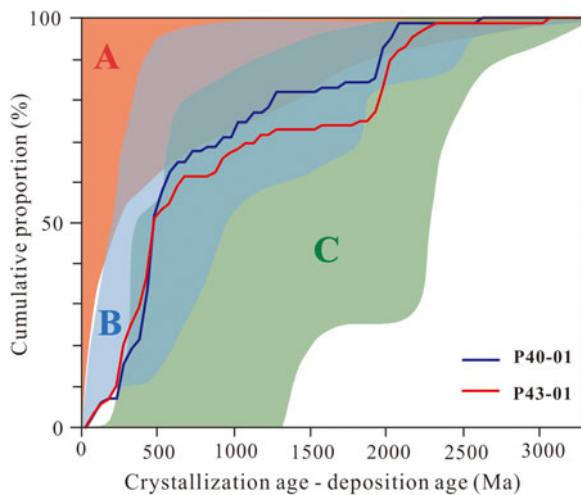


Fig. 18. (Colour online) Variation of the differences between the crystallization ages of detrital zircons and the depositional age of the sedimentary sequences, plotted as cumulative proportion curves (after Cawood *et al.* 2012). A – convergent setting; B – collisional setting; C – extensional setting.

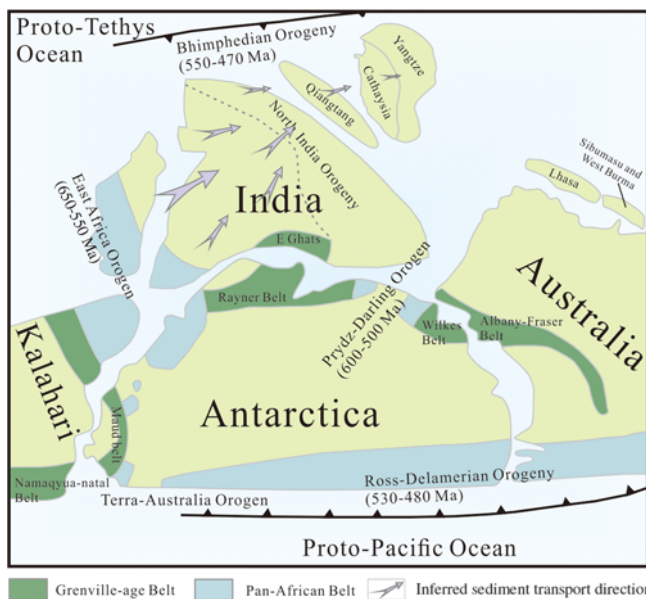


Fig. 19. (Colour online) Reconstruction of East Gondwana showing hypothetical palaeo-position of Cathaysia Block during early Palaeozoic time (modified after Fitzsimons, 2000b; Zhu *et al.* 2011).

NW–W-directed transport direction towards the Cathaysia Block and further towards the Yangtze Block during early Palaeozoic time, further ruling out the presence of a Cambrian ocean basin between the Cathaysia and Yangtze blocks (Wang *et al.* 2010; Shu *et al.* 2014; Yao *et al.* 2014, 2015). In addition, if anything at all, there would be a localized depression for receiving sediments and deposition perhaps inherited from the prior plate boundary zone between the two blocks rather than an open ocean basin. However, the presence of an ocean basin would require geological evidence, but none exists. The scenario of an Atlantic-type ocean basin (or a young and small Red-Sea-like basin) would require seafloor basaltic volcanism, but there is no evidence of this. The scenario of a back-arc basin would be the same or similar. The scenario of a Pacific-type oceanic basin would require trenches

and volcanic arcs, but there is no geological evidence of these. A Philippine-Sea-type basin would also require seafloor basaltic magmatism and subduction-zone magmatism, but again there is no evidence. Importantly, if there was an open ocean basin, then this basin would never have closed without subduction zones within it; however, there is no geological record for this speculation (trenches, thickened flyschs, arc volcanic rocks, etc.).

5.d. Palaeo-position of the Cathaysia Block in Gondwana

The palaeo-position of the Cathaysia Block within the Gondwana supercontinent has long been debated (Cawood *et al.* 2007, 2013; Li *et al.* 2010, 2014; Duan *et al.* 2011; Wang *et al.* 2011; Xu *et al.* 2013, 2016; Yao *et al.* 2014). Because unequivocal Pan-African magmatic or metamorphic rocks have been found in the SCB, the predominant Pan-African ages displayed in the age spectra of late Neoproterozoic – early Cambrian sedimentary rocks from the Cathaysia Block should indicate a Gondwana affinity (Fig. 15a,b). The Pan-African Event is widely distributed in the East African Orogen (650–550 Ma), which uplifted during the Neoproterozoic and provided zircons to the Tethyan Himalaya (DeCelles *et al.* 2000), the Prydz-Darling Orogen (600–500 Ma) of the NE margin of Antarctica (Cawood *et al.* 2007), the younger Bhimphedian Orogeny (550–470 Ma) of the North India Orogen (Cawood *et al.* 2007) and the Ross-Delamerian Orogeny (530–480 Ma) of the Terra-Australia Orogen along the Pacific margin (Cawood, 2005; Cawood *et al.* 2007). However, the specific location of the Cathaysia Block near NW India or Western Australia remains unknown.

Detrital zircon age spectra comparison has increasingly been used for correlating individual continental blocks. Some studies have suggested that the Cathaysia Block was situated near Western Australia mainly based on detrital zircons from Hainan Island, which has normally been considered as the southern extent of the Cathaysia Block (Zhou *et al.* 2015; Chen *et al.* 2017). However, there remains doubt as to whether Hainan Island should be regarded as part of the Cathaysia Block during Neoproterozoic and early Palaeozoic time (Xu *et al.* 2001, 2007, 2014b; Wan *et al.* 2007; Xia *et al.* 2012, 2018; Niu *et al.* 2015). The proposed Western Australia connection with the Cathaysia Block based on limited data therefore needs to be reconsidered. Here we compare the updated detrital zircon age spectra in the Cathaysia Block (exclude Hainan Island) with those of potential neighbouring blocks during late Neoproterozoic and early Palaeozoic time (including Qiangtang, northern India, the Lhasa Terrane and Western Australia; Fig. 15) for a better understanding of the palaeo-position of the Cathaysia Block within the Gondwana supercontinent.

The age spectra of the Cathaysia Block are consistent with similar-aged sedimentary rocks from Qiangtang and the western part of the northern India margin, particularly with the predominant Grenvillian peak at *c.* 0.95 Ga, Pan-African ages of 0.50–0.65 Ga and global crustal growth peak at *c.* 2.5 Ga (Fig. 15a–e). The Grenvillian peak gradually changed to *c.* 1100 Ma in much of the central to east northern India margin (Fig. 15f,g) and then to *c.* 1200 Ma in the Lhasa Terrane and Western Australia (Fig. 15h,i). From U–Pb and Hf isotopic data analysis, Zhu *et al.* (2011) argued that the Lhasa Terrane should have been at the northwestern margin of Australia during late Precambrian – early Palaeozoic time, rather than part of the Qiangtang–Himalaya continental margin system. The Cathaysia Block therefore seemed to be nearer Qiangtang and the western part of the northern India margin during late Neoproterozoic and Cambrian time, but was unlikely to have had a direct connection with the Lhasa Terrane

and Western Australia (Fig. 19). Furthermore, the Hf isotopic compositions of the zircons with the Pan-African ages in the Cathaysia Block show the same patterns as those in the Himalaya regions of India and Qiangtang, including the commonly positive $\epsilon_{\text{Hf}}(t)$ values at c. 650–570 Ma (Fig. 8a,b). The palaeocurrent directions from the SCB and India are consistent with this interpretation, which would have led to the detrital zircons associated with the Pan-African and Grenvillian ages transporting into the SCB (Myrow *et al.* 2003, 2006; Wang *et al.* 2010; Shu *et al.* 2014; Yao *et al.* 2014). The Pan-African aged zircons in the Cathaysia Block were therefore most probably sourced from the East African and Bhimpedian orogens. In addition, the aforementioned proposed passive margin setting for our samples in the Cathaysia Block is consistent with the passive margin setting of northern India during late Neoproterozoic – early Palaeozoic time (Yin *et al.* 2010). The similarity of the sedimentary sequences and shallow marine faunas among the Cathaysia, Himalaya and northern India regions during late Neoproterozoic – early Palaeozoic time (McKenzie *et al.* 2011; Jiang *et al.* 2013; Hughes, 2016), and the unconformity between the Ordovician and Cambrian successions in the Yunkai Domains of eastern Cathaysia and northern India (Myrow *et al.* 2009; Xu *et al.* 2014a), further support this configuration (Fig. 19).

6. Conclusions

- (1) The whole-rock major- and trace-element compositions of the late Neoproterozoic – early Cambrian sandstones from the Cathaysia Block indicate that they were mainly derived from intermediate–felsic sources with a moderate weathering history.
- (2) The U–Pb dating results of the late Neoproterozoic – early Cambrian sandstones from the Cathaysia Block show four major age populations of c. 2.5 Ga, 1000–900 Ma (Grenvillian), 870–716 Ma (middle Neoproterozoic) and 655–532 Ma (Pan-African). Provenance analysis, together with zircon Hf-isotopic compositions and morphology, suggest that most of the zircons in our study were sourced from exotic continental terranes once connected to the Cathaysia Block.
- (3) The Cathaysia Block was a passive continental margin during late Neoproterozoic – early Cambrian time. Similar age distributions between the Cathaysia and Eastern Yangtze blocks suggest that these two blocks shared the same continent without an open ocean basin between them during Cambrian time.
- (4) Qualitative comparison of age spectra of the SCB with the potential neighbouring blocks during late Neoproterozoic and early Palaeozoic time, such as Qiangtang, northern India, the Lhasa Terrane and Western Australia, shows that the Cathaysia Block might have been near Qiangtang and the western part of the northern India margin during late Neoproterozoic and Cambrian time. This inference suggests that the Cathaysia Block did not have direct a connection with the Lhasa Terrane and Western Australia in the Gondwana reconstruction.

Supplementary material. To view supplementary material for this article, please visit <https://doi.org/10.1017/S0016756819000013>.

Author ORCIDs.  Chen Xiong, 0000-0003-3285-8717

Acknowledgments. The study was financially supported by the Open Foundation of State Key Laboratory of Oil and Gas Reservoir Geology and Exploitation (grant no. PLC201605), the National Science and Technology

Major Project (grant no. 2017ZX05008005) and the National Natural Science Foundation of China (grant no. 41872109).

References

- Bai DY, Zhou L, Wang XH and Ma TQ (2007) Geochemistry of Nanhuan-Cambrian sandstones in southeastern Hunan, and its constraints on Neoproterozoic-early Paleozoic tectonic setting of South China. *Acta Geologica Sinica* **81**, 755–71 (in Chinese with English abstract).
- Belousova EA, Griffin WL, O'Reilly SY and Fisher NI (2002) Igneous zircon: trace element composition as an indicator of source rock type. *Contributions to Mineralogy and Petrology* **143**, 602–22.
- Bingen B, Austrheim H, Whitehouse MJ and Davis WJ (2004) Trace element signature and U–Pb geochronology of eclogite-facies zircon, Bergen Arcs, Caledonides of W Norway. *Contributions to Mineralogy and Petrology* **147**, 671–83.
- Bhatia MR (1983) Plate tectonics and geochemical composition of sandstones. *Journal of Geology* **916**, 611–27.
- Bhatia MR and Crook KA (1986) Trace element characteristics of graywackes and tectonic setting discrimination of sedimentary basins. *Contributions to Mineralogy and Petrology* **92**, 181–93.
- Blichert-Toft J (2008) The Hf isotopic composition of zircon reference material 91500. *Chemical Geology* **253**, 252–7.
- Blichert-Toft J and Albarede F (1997) The Lu–Hf isotope geochemistry of chondrites and the evolution of the mantle–crust system. *Earth and Planetary Science Letters* **148**, 243–58.
- BGMRGX (Bureau of Geology Mineral Resources of Guangxi Province) (1985) *Regional Geology of the Guangxi Province*. Beijing: Geological Publishing House, 853 p. (in Chinese with English abstract).
- BGMRGZ (Bureau of Geology Mineral Resources of Guizhou Province) (1988) *Regional Geology of the Guizhou Province*. Beijing: Geological Publishing House, 698 p. (in Chinese with English abstract).
- BGMRHN (Bureau of Geology Mineral Resources of Hunan Province) (1988) *Regional Geology of the Hunan Province*. Beijing: Geological Publishing House, 719 p. (in Chinese with English abstract).
- BGMRJX (Bureau of Geology Mineral Resources of Jiangxi Province) (1984) *Regional Geology of the Jiangxi Province*. Beijing: Geological Publishing House, 921 p. (in Chinese with English abstract).
- Cawood PA (2005) Terra Australis Orogen: Rodinia breakup and development of the Pacific and Iapetus margins of Gondwana during the Neoproterozoic and Paleozoic. *Earth-Science Reviews* **69**, 249–79.
- Cawood PA, Hawkesworth CJ and Dhuime B (2012) Detrital zircon record and tectonic setting. *Geology* **40**, 875–8.
- Cawood PA, Johnson MRW and Nemchin AA (2007) Early Palaeozoic orogenesis along the Indian margin of Gondwana: tectonic response to Gondwana assembly. *Earth and Planetary Science Letters* **255**, 70–84.
- Cawood PA and Nemchin AA (2000) Provenance record of a rift basin: U/Pb ages of detrital zircons from the Perth basin, western Australia. *Sedimentary Geology* **134**, 209–34.
- Cawood PA, Wang YJ, Xu YJ and Zhao GC (2013) Locating South China in Rodinia and Gondwana: a fragment of greater India lithosphere? *Geology* **41**, 903–6.
- Charvet J, Shu LS, Faure M, Choulet F, Wang B, Lu HF and Breton NL (2010) Structural development of the lower Paleozoic belt of South China: genesis of an intracontinental orogen. *Journal of Asian Earth Sciences* **39**, 309–30.
- Chen HD, Hou MC, Xu XS and Tian JC (2006) Tectonic evolution and sequence stratigraphic framework in south China during Caledonian. *Journal of Chengdu University of Technology* **33**, 1–8.
- Chen Q, Sun M, Long X, Zhao G, Wang J, Yu Y and Yuan C (2017) Provenance study for the Paleozoic sedimentary rocks from the west Yangtze Block: constraint on possible link of South China to the Gondwana supercontinent reconstruction. *Precambrian Research* **309**, 271–89.
- Concepcion RAB, Dimalanta CB, Yumul GP Jr, Faustino Eslava DV, Queano KL, Tamayo RA Jr and Imai A (2012) Petrography, geochemistry, and tectonics of a rifted fragment of Mainland Asia: evidence from the Lasala Formation, Mindoro Island, Philippines. *International Journal of Earth Sciences* **101**, 273–90.

- Condie KC (1993) Chemical composition and evolution of the upper continental crust: contrasting results from surface samples and shales. *Chemical Geology* **104**, 1–37.
- Cullers RL (1994) The controls on the major and trace element variation of shales, siltstones, and sandstones of Pennsylvanian-Permian age from uplifted continental blocks in Colorado to platform sediment in Kansas, USA. *Geochimica et Cosmochimica Acta* **58**, 4955–72.
- DeCelles PG, Gehrels GE, Quade J, Lareau B and Spurlin M (2000) Tectonic implications of U–Pb zircon ages of the Himalayan orogenic belt in Nepal. *Science* **288**, 497–9.
- Dong CY, Li C, Wan YS, Wang W, Wu YW, Xie HQ and Liu DY (2011) Detrital zircon age model of Ordovician Wenquan quartzite south of Lungmuco-Shuanghu suture in the Qiangtang area, Tibet: constraint on tectonic affinity and source regions. *Science China Earth Sciences* **54**, 1034–42.
- Dong X, Zhang ZM and Santosh M (2010) Zircon U–Pb chronology of the Nyingtri Group, southern Lhasa Terrane, Tibetan Plateau: implications for Grenvillian and Pan-African provenance and Mesozoic–Cenozoic metamorphism. *Journal of Geology* **118**, 677–90.
- Duan L, Meng QR, Zhang CL and Liu XM (2011) Tracing the position of the South China Block in Gondwana: U–Pb ages and Hf isotopes of Devonian detrital zircons. *Gondwana Research* **19**, 141–9.
- Fedo CM, Nesbitt HW and Young GM (1995) Unraveling the effects of potassium metasomatism in sedimentary rocks and paleosols, with implications for paleoweathering conditions and provenance. *Geology* **23**, 921–4.
- Fedo CM, Sircombe KN and Rainbird RH (2003) Detrital zircon analysis of the sedimentary record. *Reviews in Mineralogy and Geochemistry* **53**, 277–303.
- Fitzsimons ICW (2000a) A review of tectonic events in the East Antarctic Shield and their implications for Gondwana and earlier supercontinents. *Journal of African Earth Sciences* **31**, 3–23.
- Fitzsimons ICW (2000b) Grenville-age basement provinces in East Antarctica: evidence for three separate collisional orogens. *Geology* **28**, 879–82.
- Floyd PA and Leveridge BE (1987) Tectonic environment of the Devonian Gramscatho basin, south Cornwall: framework mode and geochemical evidence from turbiditic sandstones. *Journal of the Geological Society* **144**, 531–42.
- Floyd PA, Winchester JA and Park RG (1989) Geochemistry and tectonic setting of Lewisian clastic metasediments from the early Proterozoic Lock Marie Group of Gairloch, Scotland. *Precambrian Research* **45**, 203–14.
- Fralick PW and Kronberg BI (1997) Geochemical discrimination of clastic sedimentary rock sources. *Sedimentary Geology* **113**, 111–24.
- Gao S, Yang J, Zhou L, Li M, Hu ZC, Guo JL, Yuan HL, Gong HJ, Xiao GQ and Wei JQ (2011) Age and growth of the Archean Kongling terrain, South China, with emphasis on 3.3 Ga granitoid gneisses. *American Journal of Science* **311**, 153–82.
- Griffin WL, Belousova EA, Shee SR, Pearson NJ and O'Reilly SY (2004) Archean crustal evolution in the northern Yilgarn Craton: U–Pb and Hf-isotope evidence from detrital zircons. *Precambrian Research* **131**, 231–82.
- Griffin WL, Pearson NJ, Belousova EA, Jackson SE, Achterbergh EV, O'Reilly SY and Shee SR (2000) The Hf isotope composition of cratonic mantle: LAM–MC–ICPMS analysis of zircon megacrysts in kimberlites. *Geochimica et Cosmochimica Acta* **64**, 133–47.
- Griffin WL, Wang X and Jackson SE (2002) Zircon chemistry and magma genesis, SE China: in-situ analysis of Hf isotopes, Tonglu and Pingtan igneous complexes. *Lithos* **61**, 237–69.
- Gu XX, Liu JM, Zheng MH, Tang JX and Qi L (2002) Provenance and tectonic setting of the Proterozoic turbidites in Hunan, South China: geochemical evidence. *Journal of Sedimentary Research* **72**, 393–407.
- Guo JL, Gao S, Wu YB, Li M, Chen K, Hu ZC, Liang ZW, Liu YS, Zhou L, Zong KQ, Zhang W and Chen HH (2014) 3.45 Ga granitic gneisses from the Yangtze Craton, South China: implications for Early Archean crustal growth. *Precambrian Research* **242**, 82–95.
- Guo L, Zhang HF, Harris N, Xu WC and Pan FB (2017) Detrital zircon U–Pb geochronology, trace-element and Hf isotope geochemistry of the metasedimentary rocks in the eastern Himalayan syntaxis: tectonic and paleogeographic implications. *Gondwana Research* **41**, 207–21.
- Guo LZ, Shi YS, Ma RS, Lu HF and Ye SF (1985) Plate movement and crustal evolution of the Jiangnan Proterozoic mobile belt, Southeast China. *Earth Science (Chikyū Kagaku)* **39**, 156–66.
- He SP, Li RS, Wang C, Zhang HF, Ji WH, Yu PS, Gu PY and Shi C (2011) Discovery of 4.0 Ga detrital zircons in the Changdu Block, North Qiangtang, Tibetan Plateau. *Chinese Science Bulletin* **56**, 647–58.
- Hidaka H, Shimizu H and Adachi M (2002) U–Pb geochronology and REE geochemistry of zircons from Palaeoproterozoic paragneiss clasts in the Mesozoic Kamiaso conglomerate, central Japan: evidence for an Archean provenance. *Chemical Geology* **187**, 279–93.
- Hoskin PWO and Schaltegger U (2003) The composition of zircon and igneous and metamorphic petrogenesis. *Reviews in Mineralogy and Geochemistry* **53**, 27–62.
- Hu ZC, Liu YS, Gao S, Liu WG, Zhang W, Tong XR, Lin L, Zong KQ, Li M and Chen HH (2012) Improved in situ Hf isotope ratio analysis of zircon using newly designed X skimmer cone and jet sample cone in combination with the addition of nitrogen by laser ablation multiple collector ICP-MS. *Journal of Analytical Atomic Spectrometry* **27**, 1391–9.
- Huang K, Opdyke ND and Zhu R (2000) Further paleomagnetic results from the Silurian of the Yangtze Block and their implications. *Earth and Planetary Science Letters* **175**, 191–202.
- Hughes NC (2016) The Cambrian palaeontological record of the Indian subcontinent. *Earth-Science Reviews* **159**, 428–61.
- Jiang B, Sinclair HD, Niu Y and Yu J (2013) Late Neoproterozoic-early Paleozoic evolution of the South China Block as a retroarc thrust wedge/foreland basin system. *International Journal of Earth Sciences* **103**, 23–40.
- Leier AL, Kapp P, Gehrels GE and DeCelles PG (2007) Detrital zircon geochronology of Carboniferous–Cretaceous strata in the Lhasa Terrane, Southern Tibet. *Basin Research* **19**, 361–78.
- Li XH (1997) Timing of the Cathaysia Block formation: constraints from SHRIMP U–Pb zircon geochronology. *Episodes* **20**, 188–92.
- Li XH, Li ZX and Li WX (2014) Detrital zircon U–Pb age and Hf isotope constraints on the generation and reworking of Precambrian continental crust in the Cathaysia Block, South China: a synthesis. *Gondwana Research* **25**, 1202–15.
- Li ZX, Evans DAD and Zhang S (2004) A 90 degrees spin on Rodinia: possible causal links between the Neoproterozoic supercontinent, superplume, true polar wander and low-latitude glaciation. *Earth and Planetary Science Letters* **220**, 409–21.
- Li ZX, Li XH, Wartho JA, Clark C, Li WX, Zhang CL and Bao CM (2010) Magmatic and metamorphic events during the early Paleozoic Wuyi–Yunkai orogeny, southeastern South China: new age constraints and pressure–temperature conditions. *Geological Society of America Bulletin* **122**, 772–93.
- Liu BJ and Xu XS (1994) *Atlas of Lithofacies and Palaeogeography of South China (Sinian to Triassic)*. Beijing: Science Press, 188 p.
- Liu R, Zhou HW, Zhang L, Zhong ZQ, Zeng W, Xiang H, Jin S, Lu XQ and Li CZ (2009) Paleoproterozoic reworking of ancient crust in the Cathaysia Block, South China: evidence from zircon trace elements, U–Pb and Lu–Hf isotopes. *Chinese Science Bulletin* **54**, 1543–54.
- Liu YS, Hu ZC, Gao S, Gunther D, Xu J, Gao CG and Chen HH (2008) In situ analysis of major and trace elements of anhydrous minerals by LA-ICP-MS without applying an internal standard. *Chemical Geology* **257**, 34–43.
- Ludwig KR (2003) *ISOPLOT 3.00: A Geochronological Toolkit for Microsoft Excel*. California, Berkeley: Berkeley Geochronology Center, 39 p.
- Martin EL, Collins WJ and Kirkland CL (2017) An Australian source for Pacific-Gondwanan zircons: implications for the assembly of northeastern Gondwana. *Geology* **45**, 699–702.
- McKenzie NR, Hughes NC, Myrow PM, Xiao S and Sharma M (2011) Correlation of Precambrian-Cambrian sedimentary successions across northern India and the utility of isotopic signatures of Himalayan lithotectonic zones. *Earth and Planetary Science Letters* **312**, 471–83.
- McLennan SM (1989) Rare earth elements in sedimentary rocks: influence of provenance and sedimentary processes. *Reviews in Mineralogy and Geochemistry* **21**, 169–200.
- McLennan SM, Hemming S, McDaniel DK and Hannson GN (1993) Geochemical approaches to sedimentation, provenance and tectonics. *Geological Society of America* **284**, 21–40.

- McLennan SM and Taylor SR (1980) Th and U in sedimentary rocks: crustal evolution and sedimentary recycling. *Nature* **285**, 621–4.
- McQuarrie N, Robinson D, Long S, Tobgay T, Grujic D, Gehrels G and Ducea M (2008) Preliminary stratigraphic and structural architecture of Bhutan: implications for the along strike architecture of the Himalayan system. *Earth and Planetary Science Letters* **272**, 105–17.
- Metcalfe I (1996) Gondwana dispersion, Asian accretion and evolution of Eastern Tethys. *Australian Journal of Earth Sciences* **43**, 605–23.
- Myrow PM, Hughes NC, Goodge JW, Fanning CM, Williams IS, Peng SC, Bhargava ON, Parcha SK and Pogue KR (2010) Extraordinary transport and mixing of sediment across Himalayan central Gondwana during the Cambrian-Ordovician. *Geological Society of America Bulletin* **122**, 1660–70.
- Myrow PM, Hughes NC, Paulsen TS, Williams IS, Parcha SK, Thompson KR, Bowring SA, Peng SC and Ahluwalia AD (2003) Integrated tectonostratigraphic analysis of the Himalaya and implications for its tectonic reconstruction. *Earth and Planetary Science Letters* **212**, 433–41.
- Myrow PM, Hughes NC, Searle MP, Fanning CM, Peng SC and Parcha SK (2009) Stratigraphic correlation of Cambrian-Ordovician deposits along the Himalaya: implications for the age and nature of rocks in the Mount Everest region. *Geological Society of America Bulletin* **121**, 323–32.
- Myrow PM, Snell KE, Hughes NC, Paulsen TS, Heim NA and Parcha SK (2006) Cambrian depositional history of the Zaskar Valley region of the Indian Himalaya: tectonic implications. *Journal of Sedimentary Research* **76**, 364–81.
- Nesbitt HW and Young GM (1982) Early proterozoic climates and plate motions inferred from major element chemistry of lutites. *Nature* **299**, 715–7.
- Niu YL, Liu Y, Xue QQ, Shao FL, Chen S, Duan M, Guo PY, Gong HM, Hu Y, Hu ZX, Kong JJ, Li JY, Liu JJ, Sun P, Sun WL, Ye L, Xiao YY and Zhang Y (2015) Exotic origin of the Chinese continental shelf: new insights into the tectonic evolution of the western Pacific and eastern China since the Mesozoic. *Science Bulletin* **60**, 1598–616.
- Peck WH, Valley J and Wilde S (2001) Oxygen isotope ratios and rare earth elements in 3.3 to 4.4 Ga zircons: ion microprobe evidence for high $\delta^{18}\text{O}$ continental crust and oceans in the Early Archean. *Geochimica et Cosmochimica Acta* **65**, 4215–29.
- Peng S, Kusky TM, Jiang XF, Wang L and Deng WH (2012) Geology, geochemistry, and geochronology of the Miaowan ophiolite, Yangtze craton: implications for South China's amalgamation history with the Rodinian supercontinent. *Gondwana Research* **21**, 577–94.
- Pullen A, Kapp P, Gehrels GE, Ding L and Zhang QH (2011) Metamorphic rocks in central Tibet: lateral variations and implications for crustal structure. *Geological Society of America Bulletin* **123**, 585–600.
- Rainbird RH, Nesbitt HW and Donaldson JA (1990) Formation and diagenesis of a sub-Huronian saprolite: comparison with a modern weathering profile. *The Journal of Geology* **98**, 801–22.
- Roser B and Korsch R (1986) Determination of tectonic setting of sandstone-mudstone suites using SiO_2 content and $\text{K}_2\text{O}/\text{Na}_2\text{O}$ ratio. *The Journal of Geology* **94**, 635–50.
- Rubatto D (2002) Zircon trace element geochemistry: partitioning with garnet and the link between U–Pb ages and metamorphism. *Chemical Geology* **184**, 123–38.
- Rudnick R and Gao S (2003) Composition of the continental crust. *Treatise on Geochemistry* **3**, 1–64.
- Santosh M, Shaji E, Tsunogae T, Mohan MR, Satyanarayanan M and Horie K (2013) Suprasubduction zone ophiolite from Agali hill: petrology, zircon SHRIMP U–Pb geochronology, geochemistry and implications for Neoproterozoic plate tectonics in southern India. *Precambrian Research* **231**, 301–24.
- Savoy L, Stevenson RK and Mountjoy EW (2000) Provenance of upper Devonian-lower Carboniferous miogeoclinal strata, southeastern Canadian Cordillera: link between tectonics and sedimentation. *Journal of Sedimentary Research* **70**, 181–93.
- Shabeer KP, Kumar MS, Armstrong R and Buick IS (2005) Constraints on the timing of Pan-African granulite-facies metamorphism in the Kerala Khondalite Belt of southern India: SHRIMP mineral ages and Nd isotopic systematics. *The Journal of Geology* **113**, 95–106.
- Shu LS, Faure M, Yu JH and Jahn BM (2011) Geochronological and geochemical features of the Cathaysia Block (South China): new evidence for the Neoproterozoic breakup of Rodinia. *Precambrian Research* **187**, 263–76.
- Shu LS, Jahn BM, Charvet J, Santosh M, Wang B, Xu XS and Jiang SY (2014) Early Paleozoic depositional environment and intracontinental orogeny in the Cathaysia Block (South China): implications from stratigraphic, structural, geochemical and geochronologic evidence. *American Journal of Science* **314**, 154–86.
- Shu LS, Yu JH, Jia D, Wang B, Shen WZ and Zhang YQ (2008) Early Paleozoic orogenic belt in the eastern segment of South China. *Geological Bulletin of China* **27**, 1581–93 (in Chinese with English abstract).
- Shui T (1987) Tectonic framework of the southeastern China continental basement. *Scientia Sinica - Series B* **30**, 414–21 (in Chinese with English abstract).
- Singh P (2009) Major, trace and REE geochemistry of the Ganga River sediments: influence of provenance and sedimentary processes. *Chemical Geology* **266**, 242–55.
- Söderlund U, Patchett PJ, Vervoort JD and Isachsen C (2004) The ^{176}Lu decay constant determined by Lu–Hf and U–Pb isotope systematics of Precambrian mafic intrusions. *Earth and Planetary Science Letters* **219**, 311–24.
- Spencer CJ, Harris RA and Dorais MJ (2012) Depositional provenance of the Himalayan metamorphic core of Garhwal region, India: constrained by U–Pb and Hf isotopes in zircons. *Gondwana Research* **22**, 26–35.
- Sun M, Chen NS, Zhao GC, Wilde SA, Ye K, Guo JH, Chen Y and Yuan C (2008) U–Pb zircon and Sm–Nd isotopic study of the Huangtuling granulite, Dabie-Sulu belt, China: implication for the Paleoproterozoic tectonic history of the Yangtze Craton. *American Journal of Science* **308**, 469–83.
- Sun SS and McDonough WF (1989) Chemical and isotopic systematics of oceanic basalts: implications for mantle composition and processes. In: *Magmatism in the Ocean Basins* (eds AD Saunders and MJ Norry), pp. 313–45. Geological Society of London, Special Publication no. 42.
- Taylor SR and McLennan S (1985) *The Continental Crust: Its Composition and Evolution*. Oxford: Blackwell Press, 312 p.
- Veevers JJ (2007) Pan-Gondwanaland post-collisional extension marked by 650–500 Ma alkaline rocks and carbonatites and related detrital zircons: a review. *Earth-Science Reviews* **83**, 1–47.
- Veevers JJ, Saeed A, Belousova EA and Griffin WL (2005) U–Pb ages and source composition by Hf-isotope and trace-element analysis of detrital zircons in Permian sandstone and modern sand from southwestern Australia and a review of the paleogeographical and denudational history of the Yilgam craton. *Earth-Science Reviews* **68**, 245–79.
- Wan Y, Liu D, Xu M, Zhuang J, Song B, Shi Y and Du L (2007) SHRIMP U–Pb zircon geochronology and geochemistry of metavolcanic and metasedimentary rocks in Northwestern Fujian, Cathaysia Block, China: tectonic implications and the need to redefine lithostratigraphic units. *Gondwana Research* **12**, 166–83.
- Wang D, Wang XL, Zhou JC and Shu XJ (2013) Unraveling the Precambrian crustal evolution by Neoproterozoic conglomerates, Jiangnan orogen: U–Pb and Hf isotopes of detrital zircons. *Precambrian Research* **233**, 223–36.
- Wang W, Zeng MF, Zhou MF, Zhao JH, Zheng JP and Lan ZF (2018) Age, provenance and tectonic setting of Neoproterozoic to early Paleozoic sequences in southeastern South China block: constraints on its linkage to western Australia-East Antarctica. *Precambrian Research* **309**, 290–308.
- Wang XC, Li XH, Li ZX, Li QL, Tang GQ, Gao YY, Zhang QR and Liu Y (2012) Episodic Precambrian crust growth: evidence from U–Pb ages and Hf–O isotopes of zircon in the Nanhua Basin, central South China. *Precambrian Research* **222–223**, 386–403.
- Wang YJ, Zhang AM, Fan WM, Zhao GC, Zhang GW, Zhang YZ, Zhang FF and Li SZ (2011) Kwangsiian crustal anatexis within the eastern South China block: geochemical, zircon U–Pb geochronological and Hf isotopic fingerprints from the gneissoid granites of Wugong and Wuyi-Yunkai domains. *Lithos* **127**, 239–60.
- Wang YJ, Zhang F, Fan W, Zhang G, Chen S, Cawood PA and Zhang A (2010) Tectonic setting of the South China Block in the early Paleozoic: resolving intracontinental and ocean closure models from detrital zircon U–Pb geochronology. *Tectonics* **29**, 16.
- Webb AAG, Yin A and Dubey CS (2013) U–Pb zircon geochronology of major lithologic units in the eastern Himalaya: implications for the origin and

- assembly of Himalayan rocks. *Geological Society of America Bulletin* **125**, 499–522.
- Webb AAG, Yin A, Harrison TM, Celerier J, Gehrels GE, Manning CE and Grove M (2011)** Cenozoic tectonic history of the Himachal Himalaya (NW India) and its constraints on the formation mechanism of the Himalayan orogen. *Geosphere* **7**, 1013–61.
- Wiedenbeck M, Alle P, Corfu F, Griffin WL, Meier M, Oberli F, Quadt AV, Roddick JC and Spiegel W (1995)** Three natural zircon standards for U-Th-Pb, Lu-Hf, trace element and REE analyses. *Geostandards Newsletter* **19**, 1–23.
- Wu L, Jia D, Deng F and Li YQ (2010)** Provenance of detrital zircons from the late Neoproterozoic to Ordovician sandstones of South China: implications for its continental affinity. *Geological Magazine* **147**, 974–80.
- Xia Y, Xu X, Niu Y and Liu L (2018)** Neoproterozoic amalgamation between Yangtze and Cathaysia blocks: the magmatism in various tectonic settings and continent-arc-continent collision. *Precambrian Research* **309**, 56–87.
- Xia Y, Xu XS, Zhao GC and Liu L (2015)** Neoproterozoic active continental margin of the Cathaysia block: evidence from geochronology, geochemistry, and Nd–Hf isotopes of igneous complexes. *Precambrian Research* **269**, 195–216.
- Xia Y, Xu XS and Zhu KY (2012)** Paleoproterozoic S- and A-type granites in southwestern Zhejiang: magmatism, metamorphism and implications for the crustal evolution of the Cathaysia basement. *Precambrian Research* **216–219**, 177–207.
- Xiong C, Chen HD, Niu YL, Chen AQ, Zhang CG, Li F, Xu SL and Yang S (2018)** Provenance, depositional setting, and crustal evolution of the Cathaysia Block, South China: insights from detrital zircon U–Pb geochronology and geochemistry of clastic rocks. *Geological Journal*, published online 11 June 2018. doi: [10.1002/gj.3253](https://doi.org/10.1002/gj.3253).
- Xu DR, Fan WM, Liang XQ and Tang HF (2001)** Characteristics of Proterozoic metamorphic basement in Hainan Island and its implications for crustal growth: Nd and Pb isotope constraints. *Journal of China University of Geosciences* **7**, 146–57 (in Chinese with English abstract).
- Xu XS, O'Reilly S, Griffin W, Deng P and Pearson N (2005)** Relict Proterozoic basement in the Nanling Mountains (SE China) and its tectonothermal overprinting. *Tectonics* **24**, 1–16.
- Xu XS, O'Reilly S, Griffin W, Wang X, Pearson N and He Z (2007)** The crust of Cathaysia: age, assembly and reworking of two terranes. *Precambrian Research* **158**, 51–78.
- Xu XS, Xu Q and Pan GT (1996)** The Continental Evolution of Southern China and its Global Comparison. Beijing: Geological Publishing House, 161 p.
- Xu YJ, Cawood PA and Du YS (2016)** Intraplate orogenesis in response to Gondwana assembly: Kwangsi Orogeny, South China. *American Journal of Science* **316**, 329–62.
- Xu YJ, Cawood PA, Du YS, Hu LS, Yu WC, Zhu YH and Li WC (2013)** Linking South China to northern Australia and India on the margin of Gondwana: constraints from detrital zircon U–Pb and Hf isotopes in Cambrian strata. *Tectonics* **32**, 1547–58.
- Xu YJ, Cawood PA, Du YS, Huang H and Wang X (2014a)** Early Paleozoic orogenesis along Gondwana's northern margin constrained by provenance data from South China. *Tectonophysics* **636**, 40–51.
- Xu YJ, Cawood PA, Du YS, Zhong ZQ and Hughes NC (2014b)** Terminal suturing of Gondwana along the southern margin of South China Craton: evidence from detrital zircon U–Pb ages and Hf isotopes in Cambrian and Ordovician strata, Hainan Island. *Tectonics* **33**, 2490–504.
- Yan CL, Shu LS, Santosh M, Yao JL, Li JY and Li C (2015)** The Precambrian tectonic evolution of the western Jiangnan Orogen and western Cathaysia Block: Evidence from detrital zircon age spectra and geochemistry of clastic rocks. *Precambrian Research* **268**, 33–60.
- Yang Z, Sun Z, Yang T and Pei J (2004)** A long connection (750–380 Ma) between South China and Australia: paleomagnetic constraints. *Earth and Planetary Science Letters* **220**, 423–34.
- Yao JL, Shu LS and Santosh M (2011)** Detrital zircon U–Pb geochronology, Hf-isotopes and geochemistry: new clues for the Precambrian crustal evolution of Cathaysia Block, South China. *Gondwana Research* **20**, 553–67.
- Yao WH, Li ZX and Li WX (2015)** Was there a Cambrian ocean in South China? Insight from detrital provenance analyses. *Geological Magazine* **152**, 184–91.
- Yao WH, Li ZX, Li WX, Li XH and Yang JH (2014)** From Rodinia to Gondwana land: a tale from detrital provenance analyses of the Cathaysia Block, South China. *American Journal of Science* **314**, 278–313.
- Ye MF, Li XH, Li WX, Liu Y and Li ZX (2007)** SHRIMP zircon U–Pb geochronological and whole-rock geochemical evidence for an early Neoproterozoic Sibaoan magmatic arc along the southeastern margin of the Yangtze Block. *Gondwana Research* **12**, 144–56.
- Yin A, Dubey C, Webb A, Kelty T, Grove M, Gehrels GE and Burgess W (2010)** Geologic correlation of the Himalayan orogen and Indian craton. Part 1: structural geology. U–Pb zircon geochronology, and tectonic evolution of the Shillong Plateau and its neighboring regions in NE India. *Geological Society of America Bulletin* **122**, 336–59.
- Yu JH, O'Reilly SY, Wang LJ, Griffin WL, Zhang M, Wang RC, Jiang SY and Shu LS (2008)** Where was South China in the Rodinia supercontinent? Evidence from U–Pb geochronology and Hf isotopes of detrital zircons. *Precambrian Research* **164**, 1–15.
- Yu JH, O'Reilly SY, Wang L, Griffin WL, Zhou MF, Zhang M and Shu L (2010)** Components and episodic growth of Precambrian crust in the Cathaysia Block, South China: evidence from U–Pb ages and Hf isotopes of zircons in Neoproterozoic sediments. *Precambrian Research* **181**, 97–114.
- Yu JH, O'Reilly SY, Zhou MF, Griffin WL and Wang LJ (2012)** U–Pb geochronology and Hf–Nd isotopic geochemistry of the Badu Complex, Southeastern China: implications for the Precambrian crustal evolution and paleogeography of the Cathaysia Block. *Precambrian Research* **222–223**, 424–49.
- Yu JH, Wang L, O'Reilly SY, Griffin WL, Zhang M, Li C and Shu L (2009)** A Paleoproterozoic orogeny recorded in a long-lived cratonic remnant (Wuyishan terrane), eastern Cathaysia Block, China. *Precambrian Research* **174**, 347–63.
- Zhang S, Li H, Jiang G, Evans DAD, Dong J, Wu H, Yang T, Liu P and Xiao Q (2015)** New paleomagnetic results from the Ediacaran Doushantuo Formation in South China and their paleogeographic implications. *Precambrian Research* **259**, 130–42.
- Zhang SB and Zheng YF (2013)** Formation and evolution of Precambrian continental lithosphere in South China. *Gondwana Research* **23**, 1241–60.
- Zhao G and Cawood PA (2012)** Precambrian geology of China. *Precambrian Research* **222–223**, 13–54.
- Zhou MF, Yan DP, Kennedy AK, Li YQ and Ding J (2002)** SHRIMP U–Pb zircon geochronological and geochemical evidence for Neoproterozoic arc-magmatism along the western margin of the Yangtze Block, South China. *Earth and Planetary Science Letters* **196**, 51–67.
- Zhou Y, Liang XQ, Liang XR, Jiang Y, Wang C, Fu JG and Shao TB (2015)** U–Pb geochronology and Hf-isotopes on detrital zircons of Lower Paleozoic strata from Hainan Island: new clues for the early crustal evolution of southeastern South China. *Gondwana Research* **27**, 1586–98.
- Zhu DC, Zhao ZD, Niu YL, Dilek Y and Mo XX (2011)** Lhasa terrane in southern Tibet came from Australia. *Geology* **39**, 727–30.
- Zong KQ, Klemd R, Yuan Y, He ZY, Guo JL, Shi XL, Liu YS, Hu ZC and Zhang ZM (2017)** The assembly of Rodinia: the correlation of early Neoproterozoic (ca.900Ma) high-grade metamorphism and continental arc formation in the southern Beishan Orogen, southern Central Asian Orogenic Belt (CAOB). *Precambrian Research* **290**, 32–48.